ANTI-TUMOR-PROMOTING ACTIVITIES OF TRITERPENOID GLYCOSIDES; CANCER CHEMOPREVENTION BY SAPONINS

Takao Konoshima

Kyoto Pharmaceutical University
Misasagi, Yamashina-ku
Kyoto 607, Japan

INTRODUCTION

The mechanism of chemical carcinogenesis has been explained by either a two-stage theory or a multi-stage theory which consists of initiation, promotion and progression stages.[1] In these stages, the promotion stage is long-term and reversible reaction, and the development of anti-tumor-promoters has been regarded as the most effective method for the chemoprevention of cancer.

We have been extremely interested in the chemoprevention of cancer by natural products. As a continuation of our chemical and biological studies on the potential anti-tumor-promoters (chemopreventive agents), we carried out a primary screening of many kinds of natural products (flavonoids, quinones, triterpenoids, alkaloids, euglobals and crude drugs) using their inhibitory effects on Epstein-Barr virus early antigen (EBV-EA) activation induced by 12-*O*-tetradecanoylphorbol-13-acetate (TPA) which has been known as a strong promoter (Fig. 1).[2] And, many compounds that inhibit EBV-EA induction by TPA have been shown to act as inhibitors of tumor promotion on two-stage carcinogenesis tests *in vivo*.[3]

In this paper, the anti-tumor-promoting activities of some triterpenoid glycosides isolated from Japanese and Chinese traditional medicinal plants and their potentials for cancer chemopreventive agents are described.

SAPONINS FROM *WISTARIA BRACHYBOTRYS*

The knots of *Wistaria brachybotrys* SIEB. et ZUCC. (Leguminosae) are hard swellings or masses formed in the wood, used in Japanese folk medicine for the treatment of gastric cancer. From this knots, six new glycosides (**1**-**6**) were isolated together with three known glycosides (**7**-**9**) and four known isoflavonoids (**10**-**13**), and structures of new compounds were characterized by NMR spectra such as ^{1}H-^{1}H COSY, ^{1}H-^{13}C COSY, ^{1}H-^{13}C long range COSY and difference NOE experiments as shown in Chart 1.[4] Compounds **7**-**9** were identified with authentic samples isolated from soybeans.[5]

Saponins Used in Traditional and Modern Medicine
Edited by Waller and Yamasaki, Plenum Press, New York, 1996

Fig. 24

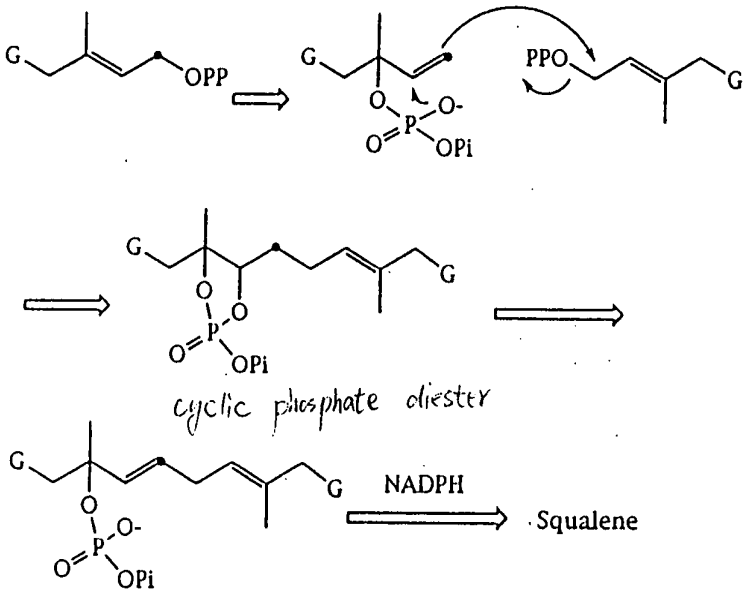

Fig. 24. Proposed mechanism of squalene formation (A)

△ 有人提出NPP券古的假說，但因獲知 Nerolidyl PP (NPP) 不是此酶基質而不成立。(cyclic phosphate diester 為其中間產物)

Fig. 25

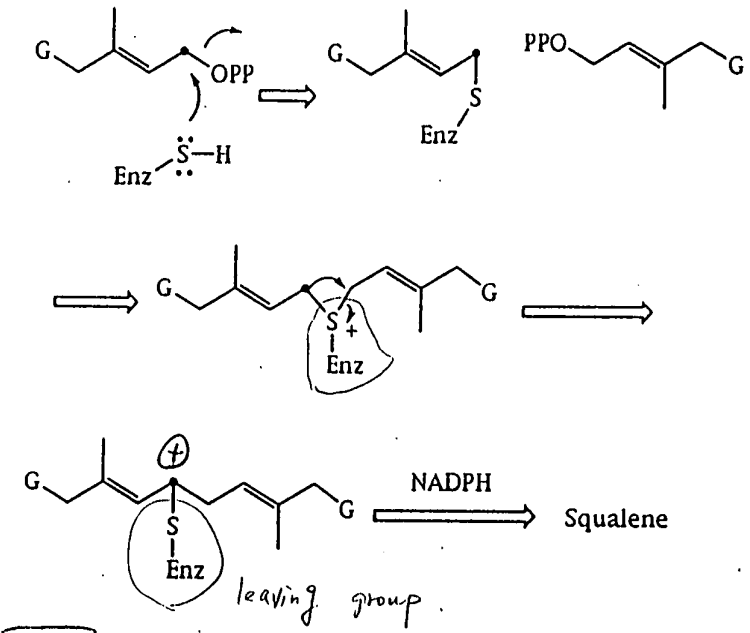

Fig. 25. Proposed mechanism of squalene formation (B)

△ 另一 Squalene 合成假說是酶活化中心有一 -SH group 券古，此酶進行類似 S_N2 之反应。

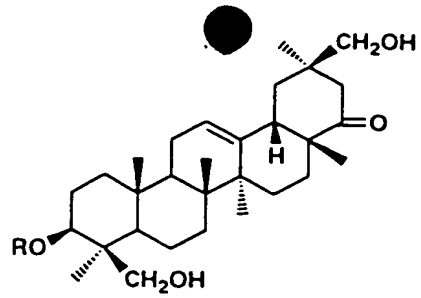

R = S_1 : wistariasaponin A (**1**)

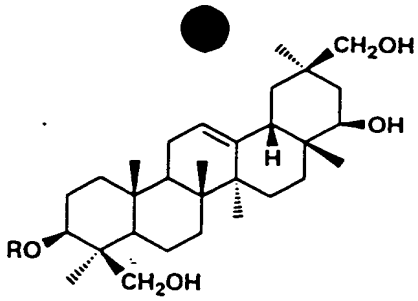

R = S_1 : wistariasaponin B_1 (**2**)
R = S_2 : wistariasaponin B_2 (**3**)

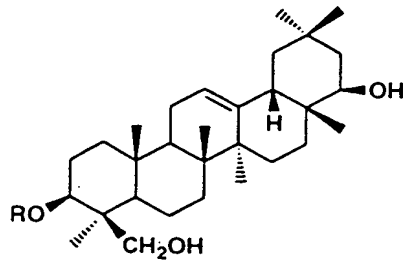

R = S_1 : wistariasaponin C (**4**)
R = S_2 : soyasaponin I (**7**)
R = S_3 : soyasaponin II (**8**)

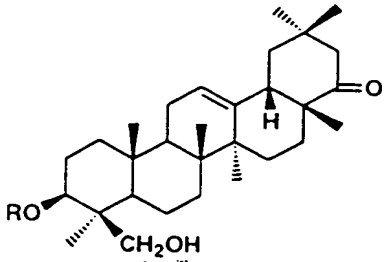

R = S_1 : wistariasaponin D (**5**)
R = S_2 : dehydrosoyasaponin I (**9**)

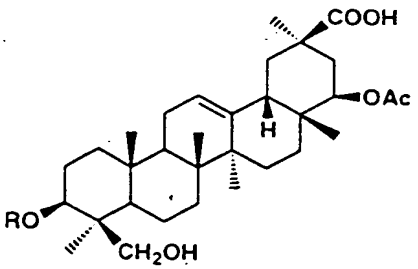

R = S_1 : wistariasaponin G (**6**)

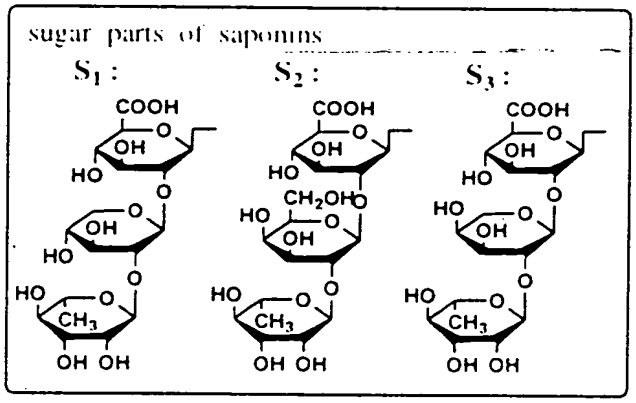

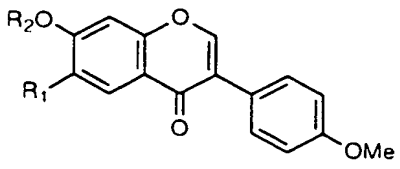

	R_1	R_2
formononetin (**10**) :	H	H
ononin (**11**) :	H	Glc
afromosin (**12**) :	OMe	H
wistin (**13**) :	OMe	Glc.

Chart 1. Saponins and Isoflavonoids from Wistaria brachybotrys

The primary screening test of these compounds was carried out utilizing a short-term *in vitro* assay on EBV-EA activation as shown in Figure 1. In this assay method, Raji cells carrying EBV genome were incubated in a medium containing *n*-butyric acid, TPA and various amounts of the test compounds. Smears were made from the cell suspension and the EBV-EA inducing cells were stained by means of an indirect immunofluorescence technique.

Lanosterol 14-Methyl demethylase

Fig. 30

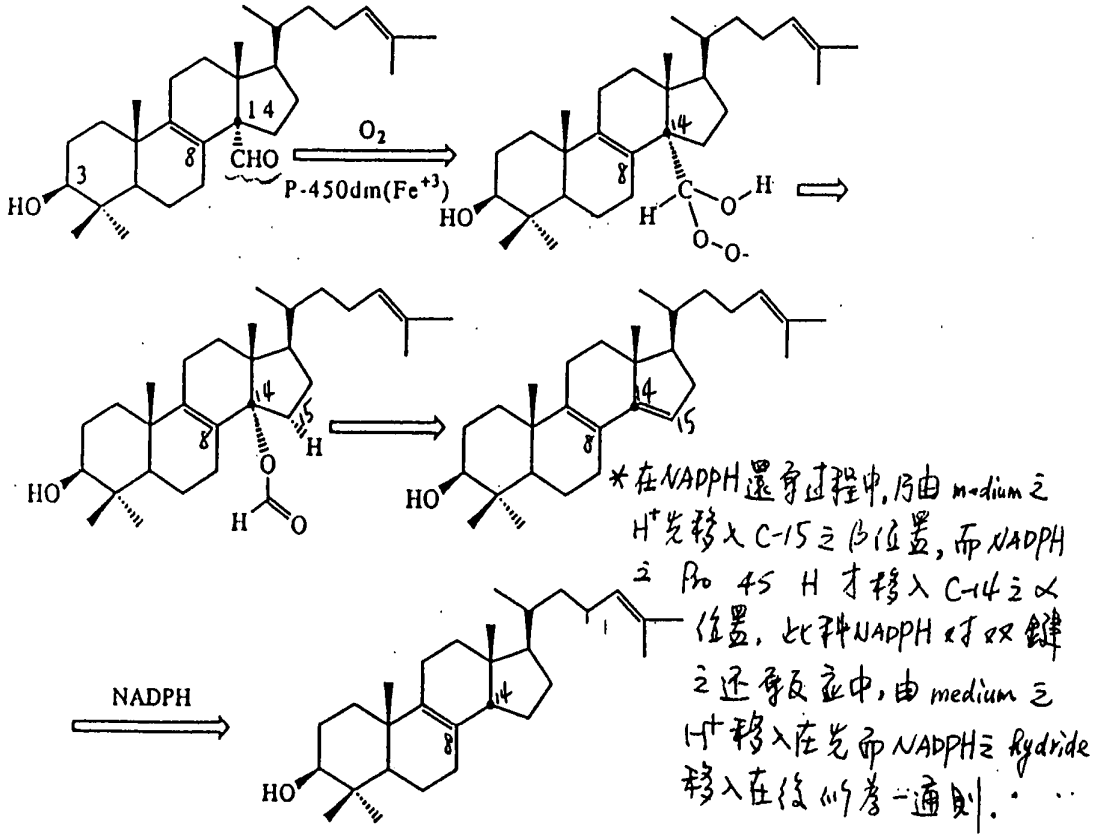

*在NADPH還原过程中，H由 medium 之 H^+ 先移入 C-15 之 β 位置，而 NADPH 之 Pro 45 H 才移入 C-14 之 α 位置，此种NADPH 对双鍵之还原反应中，由 medium 之 H+ 移入在先而 NADPH 之 hydride 移入在後的普一通則。

Demethylase inhibitors

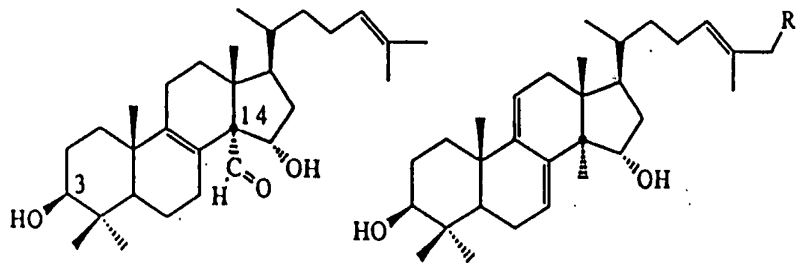

Fig. 30. Proposed mechanism of lanosterol 14-methyl demethylase.

△ Bayer Villiger reaction 之过程

Fig. 31

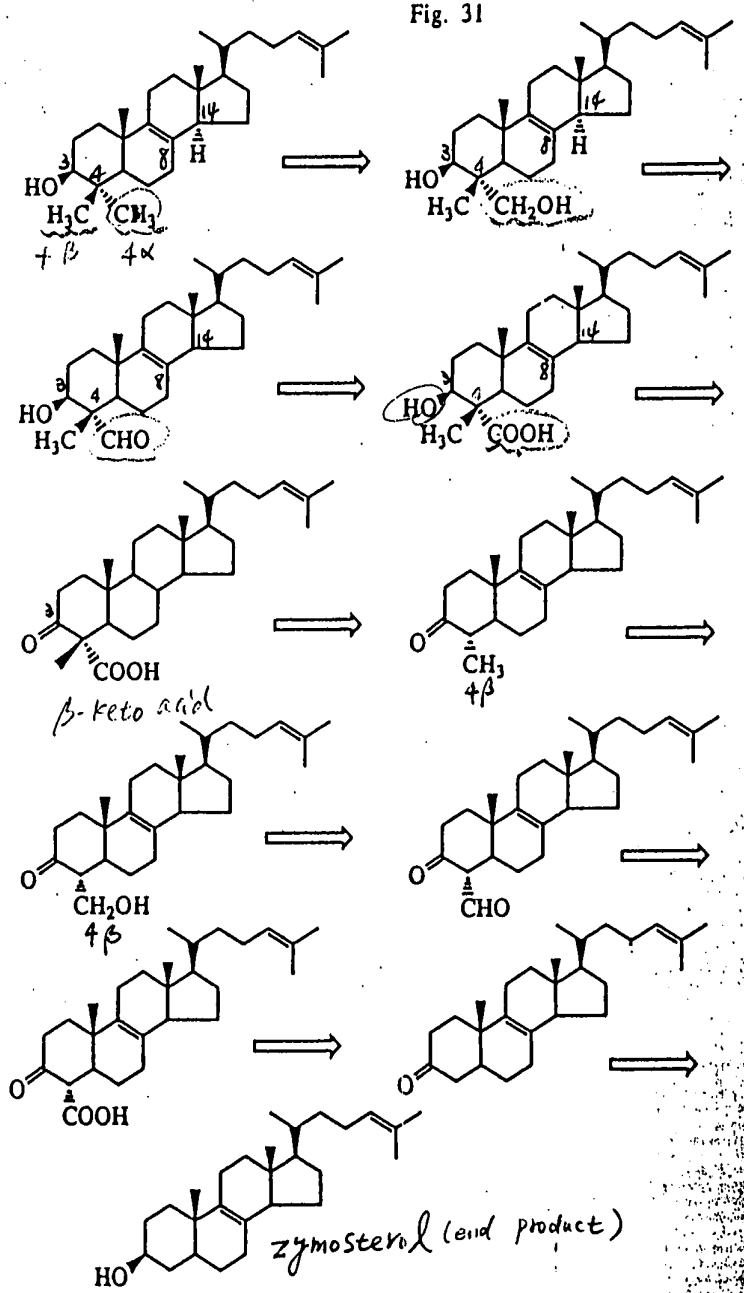

Fig. 31. 4-Methyl demethylase.

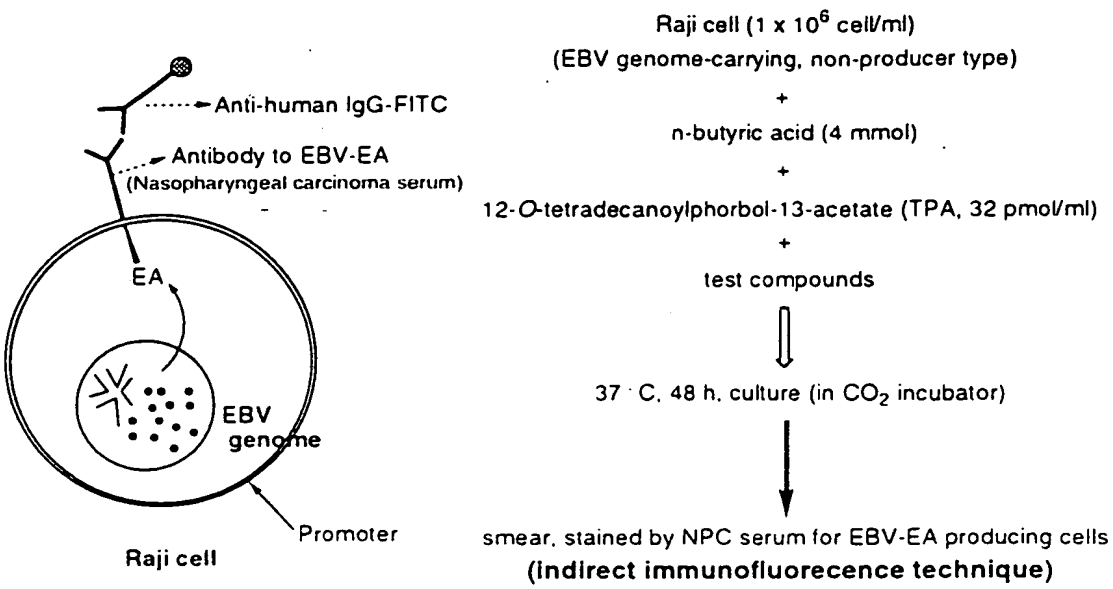

Figure 1. Method of Synergistic Assay on EBV-EA

Inhibitory effects of the constituents from *W. brachybotrys* on the EBV-EA activation and the viabilities of Raji cells used as indicator cells in this assay method are shown in Table 1.

Table 1. Percentages of EBV-EA Induction in Presence of Saponins (**1** - **9**) and Isoflavonoids (**10** - **13**) with Respect to Positive Control (100%)[1]

Sample	Concentration (mol ratio, compound/TPA)			
	1 x 10^3	5 x 10^3	1 x 10^2	1 x 10
wistariasaponin A (**1**)	---[3] (0)[2]	34.1 (70)	55.5 (>80)	80.3 (>80)
wistariasaponin B_1 (**2**)	36.8 (50)	50.7 (70)	64.3 (>80)	89.6 (>80)
wistariasaponin B_2 (**3**)	32.1 (50)	59.2 (60)	81.4 (>80)	100.0 (>80)
wistariasaponin C (**4**)	0.0 (10)	43.6 (60)	73.6 (>80)	100.0 (>80)
wistariasaponin D (**5**)	0.0 (10)	51.0 (>80)	86.1 (>80)	92.8 (>80)
wistariasaponin G (**6**)	---[3] (0)	15.4 (10)	62.6 (>80)	79.7 (>80)
soyasaponin I (**7**)	0.0 (10)	43.0 (50)	51.3 (>80)	73.0 (>80)
soyasaponin II (**8**)	0.0 (10)	45.2 (50)	67.8 (>80)	90.3 (>80)
dehydrosoyasaponin I (**9**)	50.3 (60)	67.8 (>80)	88.5 (>80)	100.0 (>80)
formononetin (**10**)	63.6 (>80)	78.8 (>80)	92.6 (>80)	100.0 (>80)
ononin (**11**)	76.0 (>80)	96.0 (>80)	100.0 (>80)	100.0 (>80)
afromosin (**12**)	36.4 (>80)	52.4 (>80)	75.8 (>80)	100.0 (>80)
wistin (**13**)	78.5 (>80)	81.5 (>80)	86.6 (>80)	100.0 (>80)
glycyrrhetic acid	15.6 (>80)	54.3 (>80)	100.0 (>80)	100.0 (>80)

[1] Values represent percentages relative to the positive control value(100%).
[2] Values in parentheses are viability percentage of Raji cells. [3] not detected.

Fig. 28

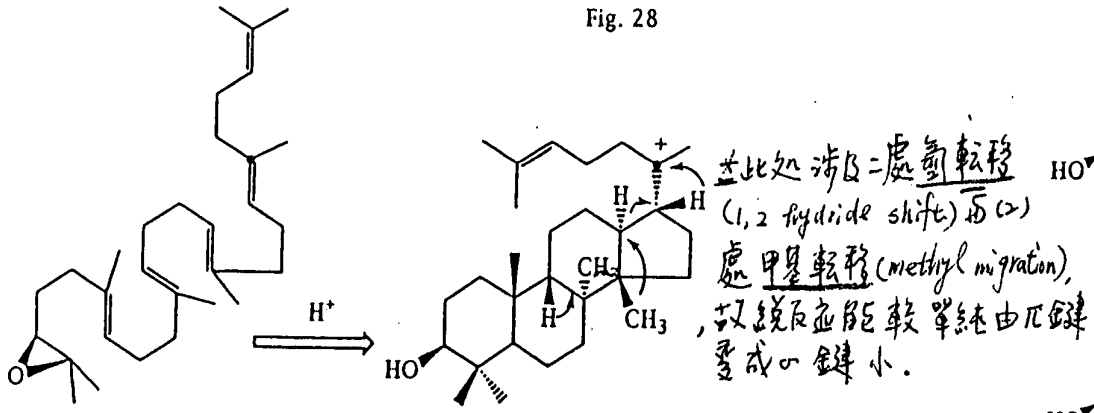

Squalene epoxide　　Protolanosterol

* 此处涉及二處氫転移 (1,2 hydride shift) 与 (2) 處甲基転移 (methyl migration), 故総反应能較單純由π鍵變成σ鍵小.

* cyclase 催反应是將雙鍵中之π鍵転化成σ鍵, 此在熱力學上顯然為一放熱反应.

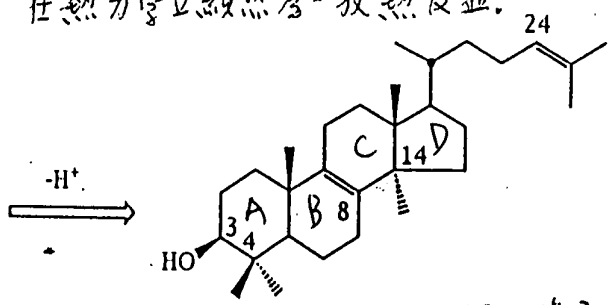

Lanosterol → 还化後再一步安定產物, 可由許多綿羊油成分之一生物原中抽取而得.

Fig. 28. Conversion of squalene epoxide to lanosterol by cyclase.

△ cyclase 將 squalene 2,3-epoxide 転化成 lanosterol, 是以限制 squalene 2,3-epoxide 之構型, 且能提供一特異之疏水性活化中心. 此活化中心含有可 protonate squalene 2,3-epoxide 之酶, 且可將基質折疊成一特定構形, 故当还化完成後 lanosterol[37] 之 4 个环 (A.B.C 而 D 環) 即已一氣呵成.

Lanosterol 14-methyl demethylase → C-14 甲基去除反应　Fig. 29

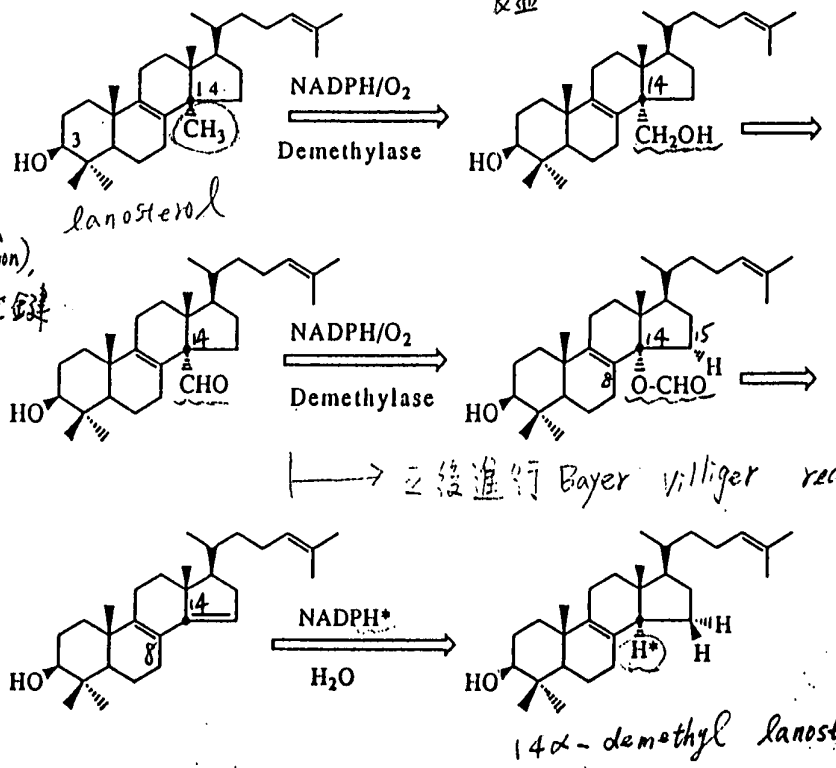

Fig. 29. Lanosterol 14-methyl demethylase.

△ 此 demethylase 為一含 P_{450} 之氧化酶, 可依序將 lanosterol 之 C-14 methyl 氧化經羥甲基与醛之階段, 推測其後是一个類似於 Bayer Villiger reaction 之述程.

△ 已知 C-14 甲基脫除过程中 C-15 之二个氫有一个要失去, 因而形成 $\Delta^{8,14}$ 共軛双鍵, 其後乃經還原 (NADPH) 考輔酶而成 14α-demethyl lanosterol

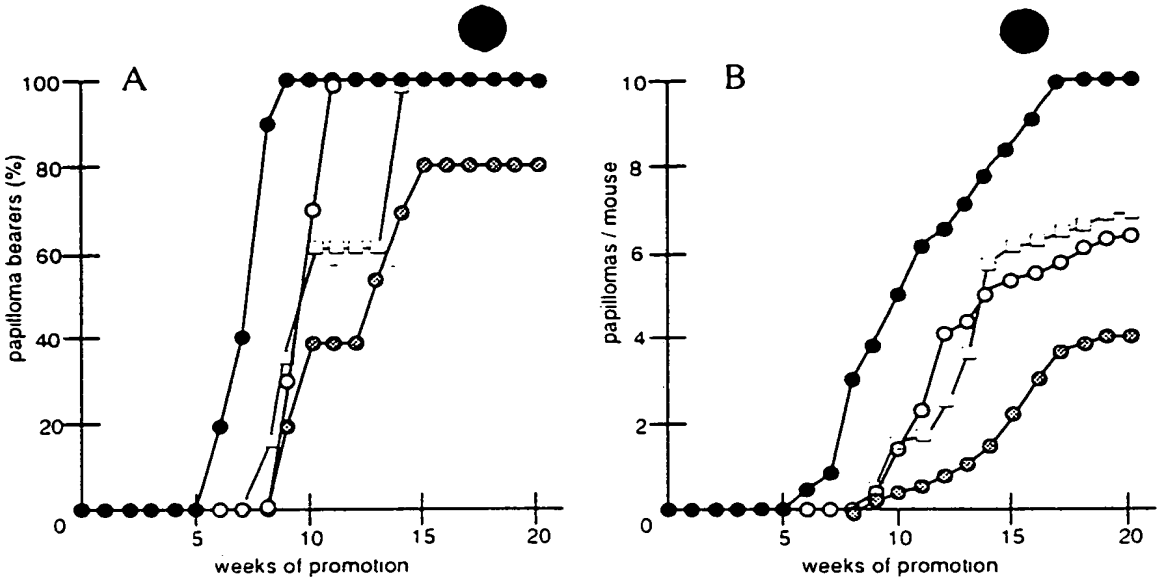

Figure 3. Inhibition of TPA-induced tumor promotion by multiple application of soyasaponin I (**7**), afromosin (**12**) and combination of **7** with **12**. Treatments of all mice were initiated with DMBA (100 μg, 394 nmol) and promoted with TPA (1 μg, 1.7 nmol) given twice weekly starting 1 week after initiation. A: Percentages of mice with papillomas. B: Average number of papillomas per mouse. ●, control TPA alone; ○, TPA + 85 nmol of soyasaponin I (**7**); □, TPA + 85 nmol of afromosin (**12**); ⊗, TPA + 42.5 nmol of soyasaponin I + 42.5 nmol of afromosin.

papillomas per mouse (about 40% reduction even at 20 weeks) (B). Furthermore, on the positive control, 100% of mice bore papillomas even at 9 weeks of promotion and more than 10 papillomas were formed per mouse after 20 weeks of promotion. In the group treated with soyasaponin I (**7**), only 20% mice bore papillomas at 9 weeks of promotion, and less than 7 papillomas were formed per mouse even at 20 weeks of promotion. And, in the group treated with isoflavone (**12**), only 30% and 60% of mice bore papillomas at 9 and 13 weeks of promotion, respectively, and less than 7 papillomas were formed per mouse at 20 weeks of promotion, as similar to **7**. Further, combined application of **7** with **12** strongly enhanced the inhibitory effects both on the rate of papilloma-bearing mice (only 40% of mice bore papillomas even at 10 weeks of promotion, and 20% reduction even at 20 weeks) and on the average number of papillomas per mouse (only 4 papillomas were formed, 60% reduction even at 20 weeks). From these facts, it was deduced that the saponin, soyasaponin I (**17**), enhanced the activity of the isoflavonoid, afromosin (**12**). These results strongly suggested that soyasaponin I (**7**) combined with afromosin (**12**) might be valuable as an antitumor promoter in two-stage chemical carcinogenesis. And these results also support the concept of synergistic effects of plural constituents in crude drugs.

SAPONINS FROM *GLEDITSIA JAPONICA* AND *GYMNOCLADUS CHINENSIS*

Gleditsia japonica MIQEL (Leguminosae) is widely distributed in Japan, and the fruits of this plant having a large amount of saponins had been used as a Japanes folk medicine for diuretic and expectorant. In these fruits, many kinds of new triterpenoid saponins and were found their strucmtures were determined by chemical and physicochemical evidences.[6] All of these

Fig. 32

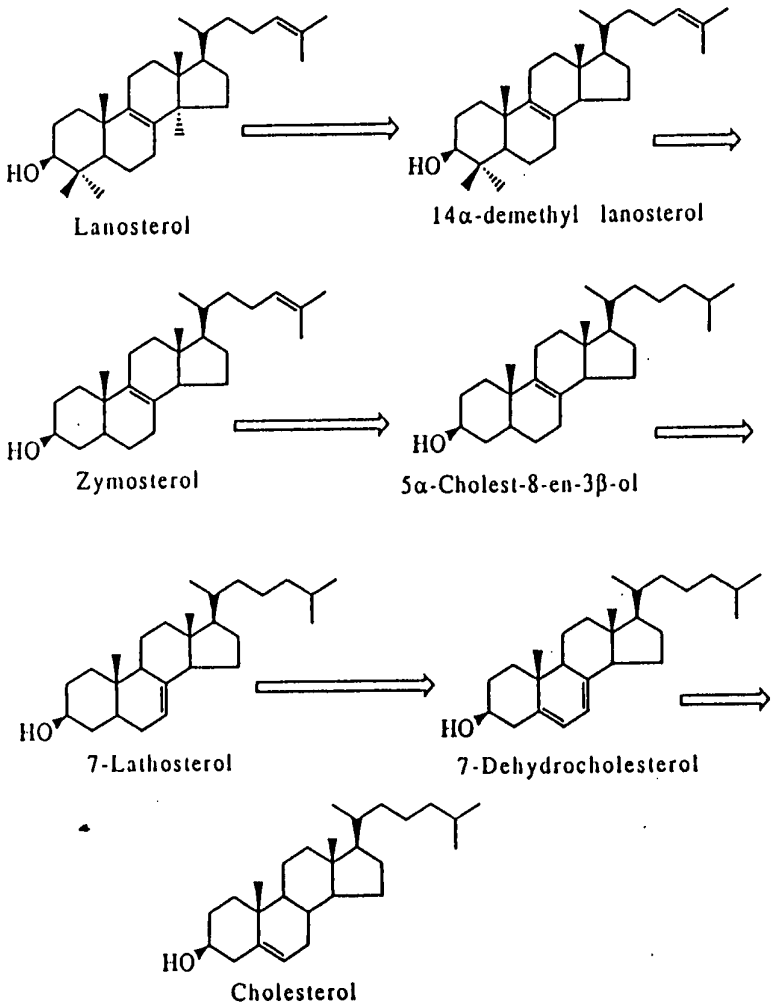

Fig. 32 Conversion of lanosterol to cholesterol.

Fig. 32 continued

Lanosterol 14-methyl demethylase

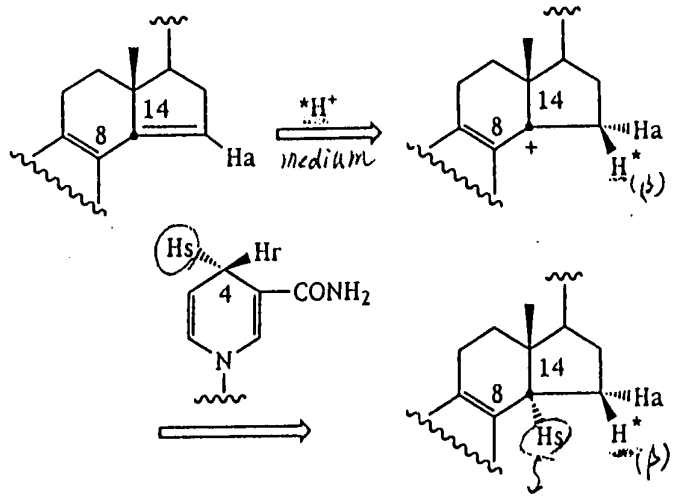

Fig. 32. continued.

Reduction of C-24 double bond

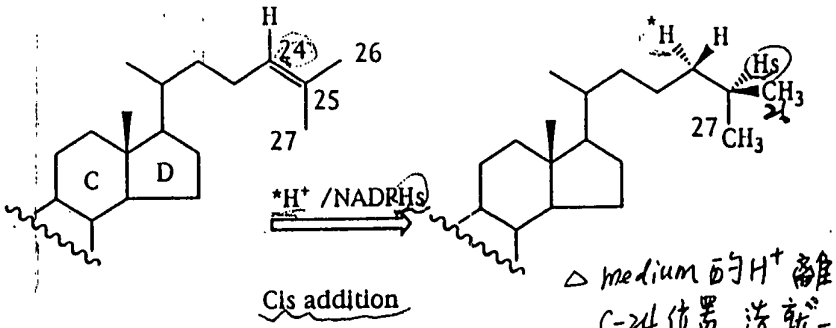

Cis addition

Fig. 33. Reduction of C-24 double bond.

Fig. 34

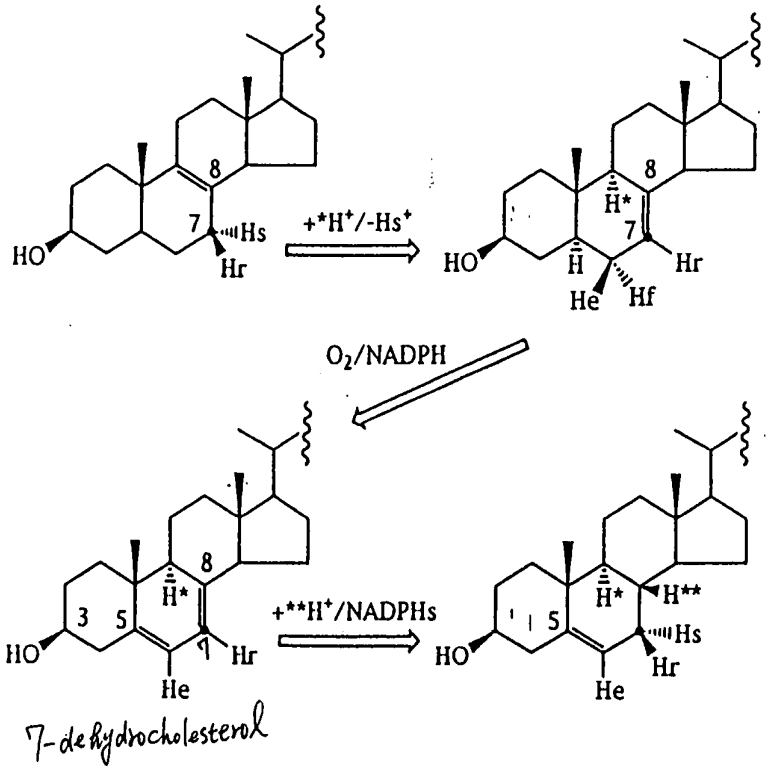

7-dehydrocholesterol

Fig. 34. The conversion of C-8 double bond to C-5 double bond in cholesterol biosynthetic pathway. An isomerization-desaturation-reduction mechanism is involved.

△ C-8 雙鍵的修飾是階段式的, C-8 雙鍵 (Δ^8 double bond) 先移至 C-7 位置 ($\Delta^8 \rightarrow \Delta^7$), 其方式顯然是 protonation-deprotonation, 其立体化學已知 deprotonation 所移去者乃 C-7 处之 Hs, 而 protonation 乃由 C-9 之雙鍵平面反方向移入, 其後 Δ^5 雙鍵乃再生成。

Of these glycosides, **1**, **6** and **7** exhibited remarkable inhibitory effects on EBV-EA activation, but **1** and **6** have strong cytotoxicities on Raji cells. Further, of the isoflavonoids, moderate activity was observed only in compound **12**. In our experiments, the remarkable inhibitory effects of soyasaponin I (**7**) and afromosin (**12**) (more than 55-47% inhibition of activation at 5 x 10^2 mol ratio/TPA and 48-24% inhibition of activation at 1 x 10^2 mol ratio/TPA) were stronger than those of glycyrrhetic acid, which is known as a strong antitumor promoter, and they preserved the high viability of Raji cells. These *in vitro* results of constituents of *Wistaria brachybotrys* strongly suggested that these compounds (**7** and **12**) might be valuable anti-tumor-promoters as well.

Therefore, the inhibitory effects of **7** and **12** on two-stage carcinogenesis of mouse skin papillomas, using dimethylbenz[*a*]anthracene (DMBA) as an initiator and TPA as a promoter, were investigated (Fig.2).

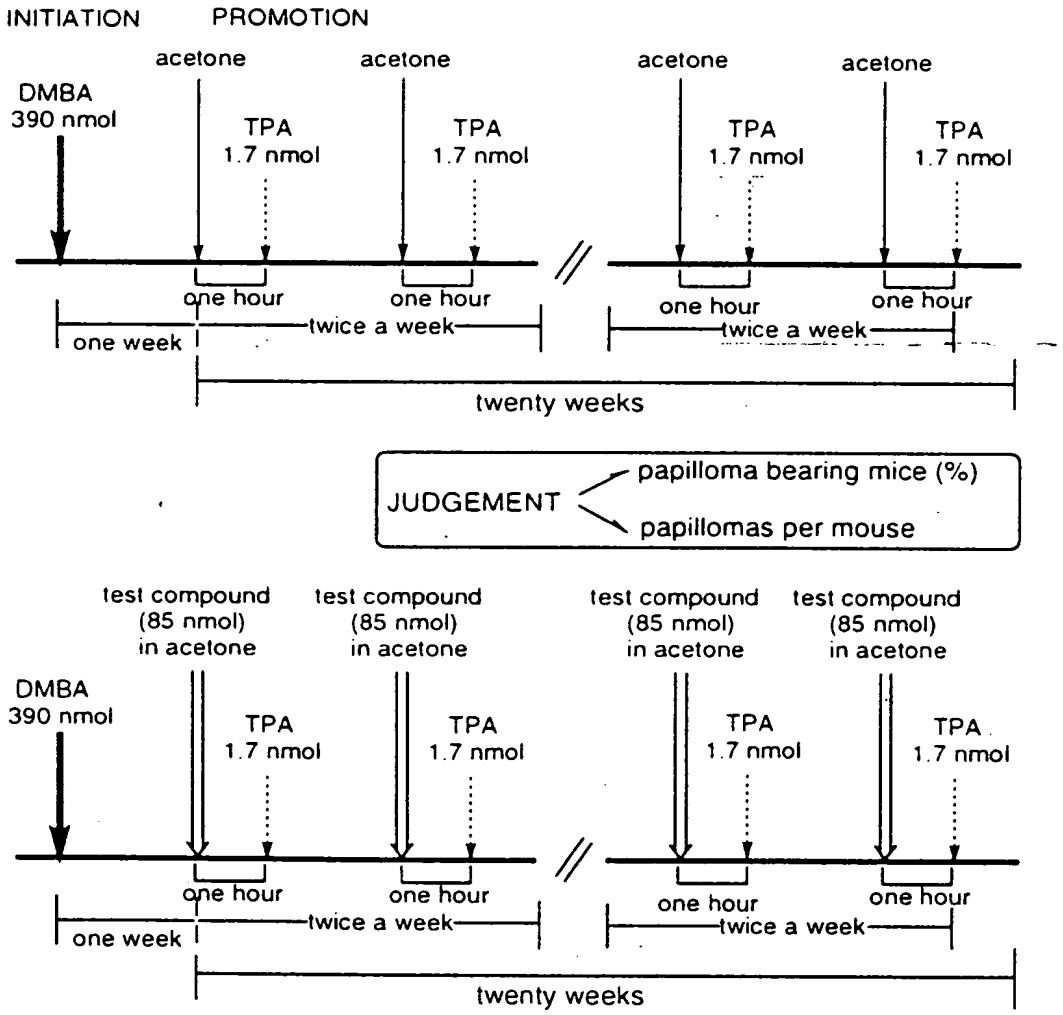

Figure 2. Method of Two-Stage Carcinogenesis Test

Because that soyasaponin I (**7**) is a major constituents and afromosin (**12**) is a major isoflavonoid in this crude drug, the combination effect of **7** with **12** was also investigated.

The inhibitory activities, evaluated by both rate (%) of mice bearing papilloma (A) and average number of papillomas per mouse (B), were compared with those of a positive control.

As shown in Figure 3, both soyasaponin I (**7**) and afromosin (**12**), when applied continuously before each TPA treatment, delayed the formation of papillomas in mouse skin as compared with the control experiment with only TPA (A), and they reduced the number of

new gleditsia saponins are 3,28-bisdesmosides of echinocystic acid, and the terminal rhamnoses of them are acylated with monoterpene carboxylic acids. And, *Gymnocladus chinensis* BAILLON (Leguminosae) close to the *Gleditsia* genus is widely distributed in south China, and the dried fruits of this plant is used as a crude drug in Chinese traditional medicine as an expectorant. This fruits also contains a large amount of saponins, and new saponins having unique structure were isolated.

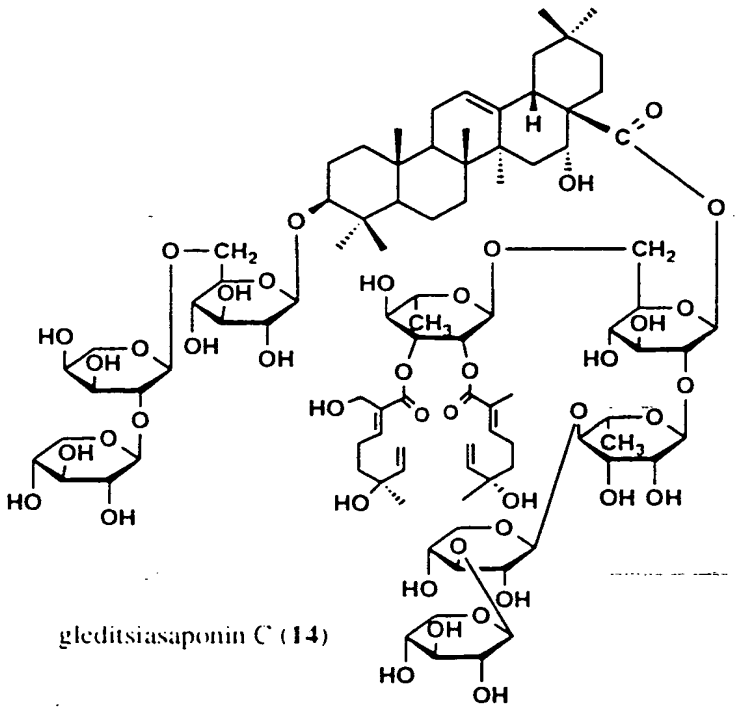

gleditsiasaponin C (14)

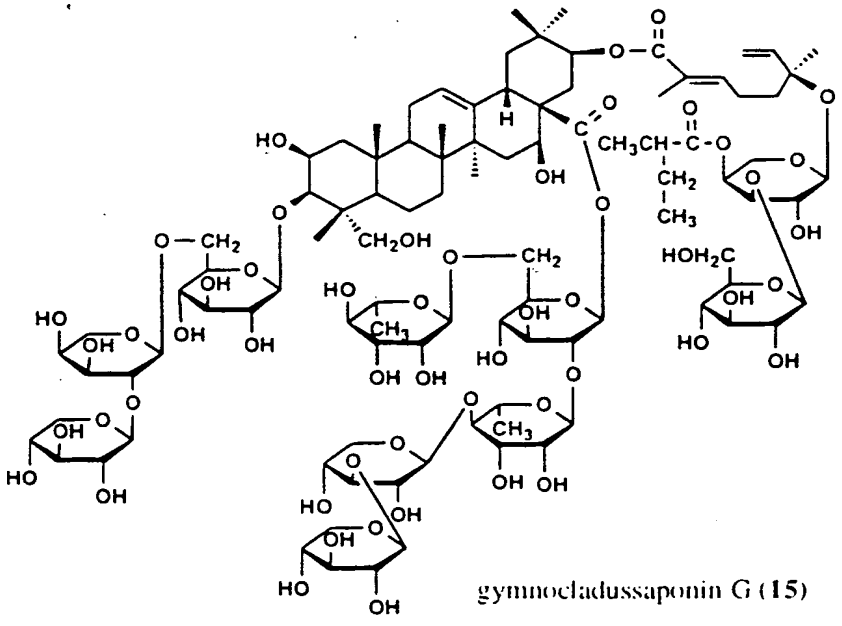

gymnocladussaponin G (15)

Chart. 2. The Structures of Gleditsia saponin C and Gymnocladus saponin G

The common sapogenin of these gymnocladus saponins is 2β,23-dihydroxy- acacic acid, and it is acylated with glycosyl monoterpene carboxylic acids. These structures were also determined by chemical and physicochemical evidence, especially NMR spectrometry.[7]

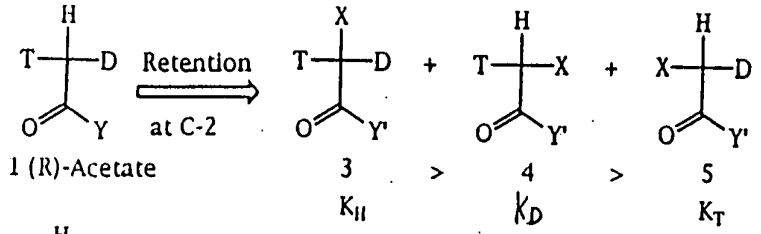

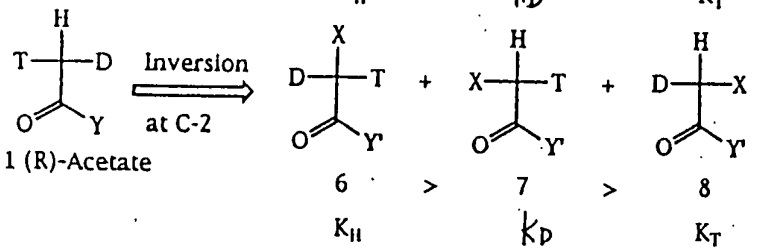

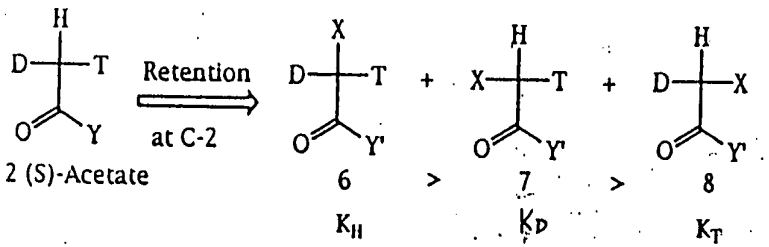

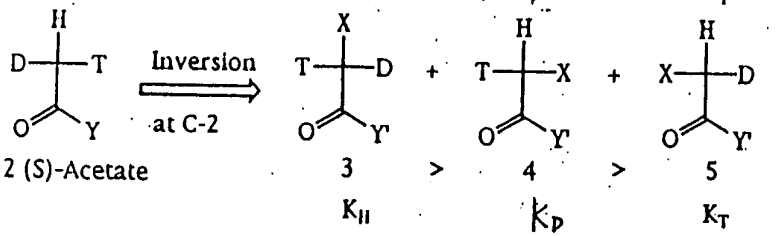

Isotope effect

$k_H > k_D > k_T$

Malate synthase (種子發芽中的enz.)

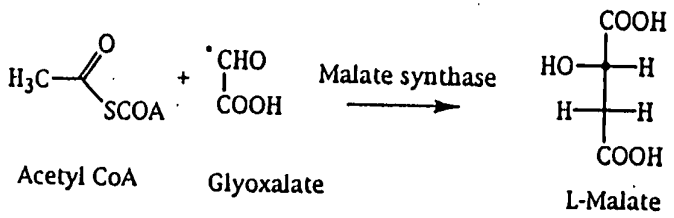

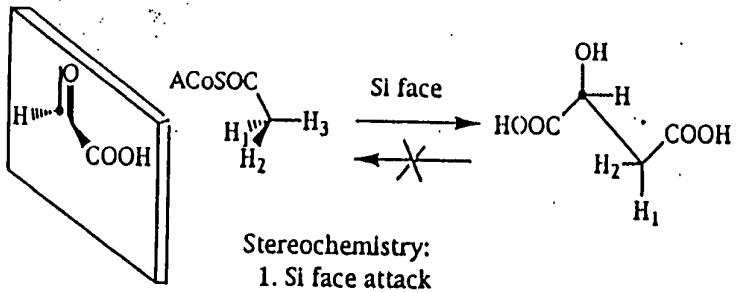

Stereochemistry:
1. Si face attack
2. Inversion at C-2 of acetyl CoA

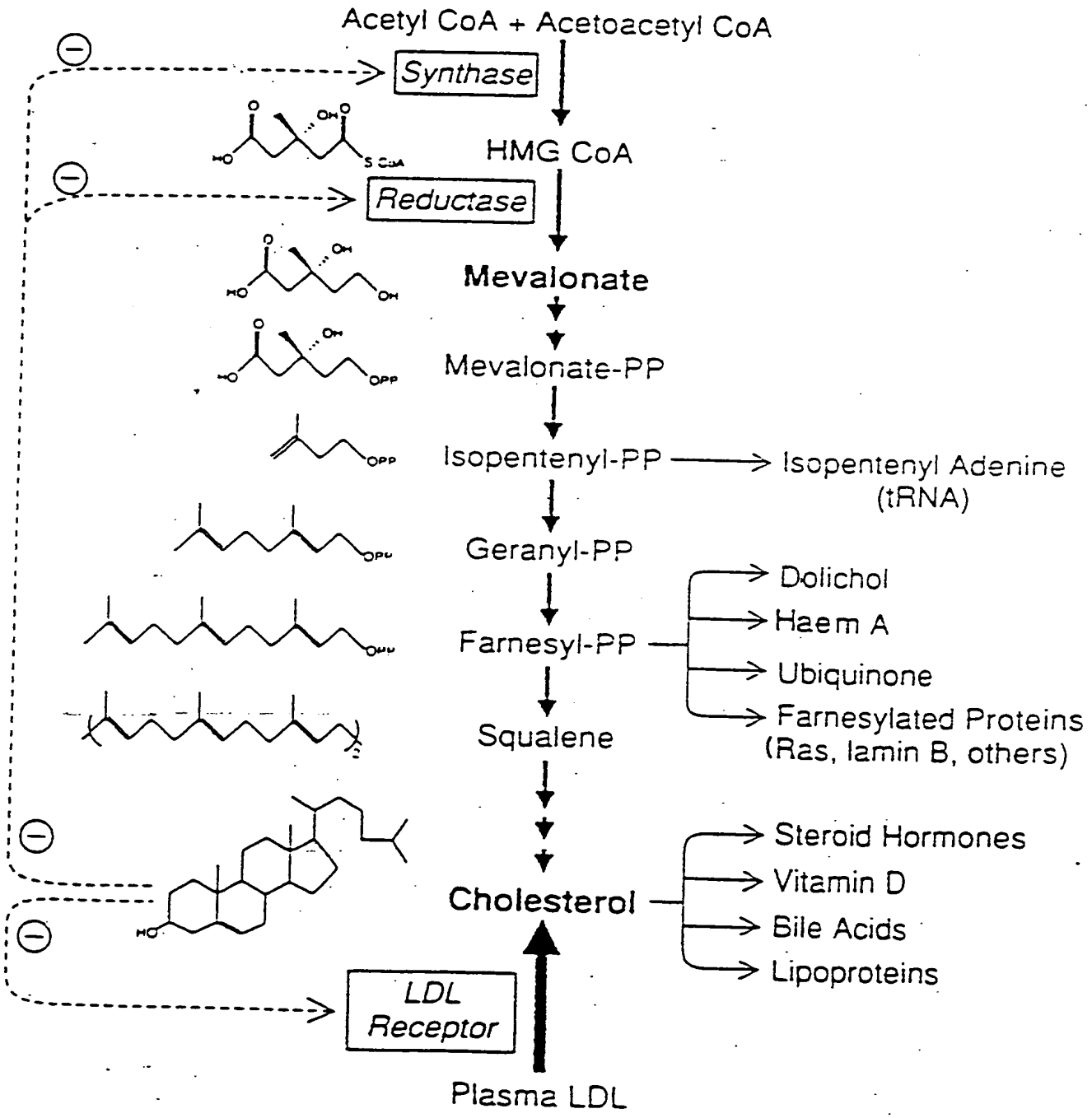
Acetyl CoA + Acetoacetyl CoA
Synthase
HMG CoA
Reductase
Mevalonate
Mevalonate-PP
Isopentenyl-PP
Isopentenyl Adenine (tRNA)
Geranyl-PP
Farnesyl-PP
Dolichol
Haem A
Ubiquinone
Farnesylated Proteins (Ras, lamin B, others)
Squalene
Cholesterol
Steroid Hormones
Vitamin D
Bile Acids
Lipoproteins
LDL Receptor
Plasma LDL

The primary screening test of these saponins on EBV-EA activation were examined, and gleditsiasaponin C (**1 4**) and gymnocladussaponin G (**1 5**) exhibited strong inhibitory effects on EBV-EA activation induced by TPA.

As shown in Table 2,* compound **1 4** exhibited moderate inhibitory effects on EBV-EA activation (about 50% inhibition at 5×10^2 mol ratio/TPA, and 40% inhibition at 1×10^2 mol ratio/TPA). Furthermore, compound **1 5** exhibited the most remarkable inhibitory effects on EBV-EA activation in these compounds obtained from *G. japonica* and *G. chinensis*. It showed more than 85% inhibition at 1×10^3 mol ratio/TPA and more than 60% inhibition even at 1×10^2 mol ratio/TPA, and preserved the high viability of Raji cells even at a high concentration. On the other hand, echinocystic acid, 3-O-glycosylechinocystic acid, desmonoterpenyl saponin C and 2β,23-dihydroxyacacic acid, showed the strong cytotoxicities on Raji cells. In our experiments, the high viability of Raji cells is beneficial for the following in vivo assay and is an important factor in developing a compound for the chemoprevention of cancer. On the basis of the results of inhibition for EBV-EA activation, the effects of saponins **1 4** and **1 5** on the two-stage carcinogenesis test of mouse skin papillomas were investigated.

Table 2. Percentages of EBV-EA Induction in Presence of Gleditsia saponins and Gymnocladus saponins with Respect to Positive Control (100%)

Sample	Concentration (mol ratio, compound/TPA)			
	1×10^3	5×10^2	1×10^2	1×10
echinocystic acid	0.0[1] (30)[2]	12.4 (40)	21.0 (60)	70.6 (>80)
echinocystic acid 3-O-glc-ara-xyl	0.0 (30)	46.5 (50)	68.2 (>80)	100.0 (>80)
desmonoterpenyl gleditsia saponin C	11.2 (10)	48.5 (40)	69.8 (70)	100.0 (>80)
gleditsia saponin C (**1 4**)	44.8 (40)	50.5 (60)	61.5 (>80)	100.0 (>80)
gleditsia saponin G	19.5 (50)	68.2 (70)	90.1 (>80)	100.0 (>80)
2β,23-dihydroxy acacic acid	21.0 (40)	43.4 (60)	60.2 (70)	100.0 (>80)
gymnocladus saponin G (**1 5**)	12.2 (70)	20.8 (70)	39.2 (70)	83.6 (>80)
gymnocladus saponin F	41.2 (60)	63.6 (70)	90.5 (70)	100.0 (>80)

[1] Values represent percentages relative to the positive control value (100%).
[2] Values in parentheses are viability percentage of Raji cells.

On the positive control, 100% of mice bore papillomas even at 6 weeks of promotion, and more than 10 papillomas were formed per mouse after 20 weeks of promotion.** When gleditsiasaponin C (**1 4**) and gymnocladussaponin G (**1 5**) was applied before each TPA treatment, they delayed the formation of papillomas and reduced the number of papillomas per mouse on mouse skin as compared with the control experiment. In the group treated with **1 4**, about 80% of mice bore papillomas at 9 weeks of promotion and 8 papillomas were formed per mouse after 20 weeks of promotion. Further, in the group treated with **1 5**, only 20% and 40% of mice bore papillomas at 8 and 9 weeks of promotion, about 80% of mice bore papillomas even

* Although many kinds of new saponins were isolated from the fruits of *G. japonica* and *G. chinensis*, other saponins showed less inhibitory effects than **1 4** and **1 5**.

** In this experiments, the SENCOR mice were used, because these species are more sensitive in the carcinogenesis test.

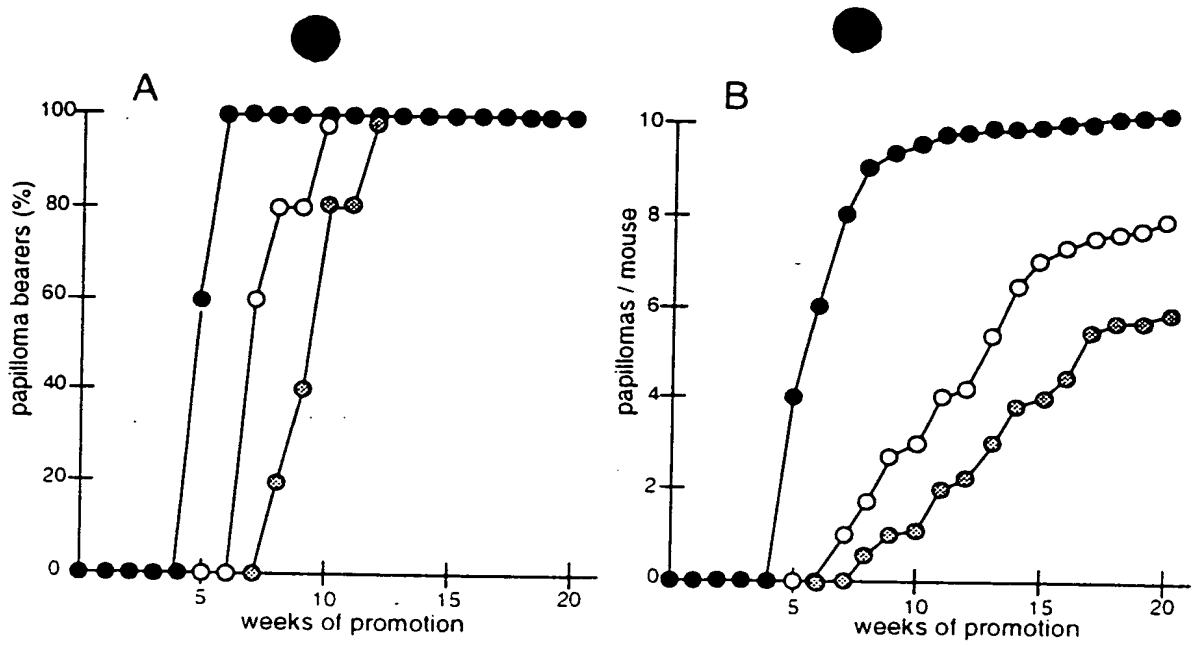

Figure 4. Inhibition of TPA-induced tumor promotion by multiple application of gleditsia saponin C (**14**) and gymnocladus saponin (**15**).
Treatments of all mice were initiated with DMBA (100 μg, 394 nmol) and promoted with TPA (1 μg, 1.7 nmol) given twice weekly starting 1 week after initiation.
A: Percentages of mice with papillomas. B: Average number of papillomas per mouse.
●, control TPA alone; , TPA + 85 nmol of gleditsia saponin C (**14**); ⊗, TPA + 85 nmol of gymnocladussaponin G (**15**)

at 11 weeks of promotion, and only 6 papillomas were formed per mouse after 20 weeks of promotion.

These results suggested that the inhibitory effects of **14** and **15** on two-stage carcinogenesis were similar to those of glycyrrhetic acid and these compounds might be valuable as antitumor promoters in chemical carcinogenesis.

SAPONINS FROM *PANAX* PLANTS

A number of damaranesaponins (ginsenosides) have been isolated from several *Panax* plants, especially from *Panax ginseng*, and also the pharmacological studies on ginseng have centered on these ginsenosides.[8] As a part of our biological studies on anti-tumor-promoters, the primary screening tests of the extracts of four crude drugs prepared from *Panax* plants was carried out. As shown in Table 3, the extract of *Panax notoginseng* exhibited significant inhibitory effects on EBV-EA activation (100% inhibition of activation at 500 μg/ml, more than 90%, 65% and 45% inhibitions at 100μg, 50 μg/ml and even at 10 μg/ml). The extract of *Panax ginseng* (steemed ginseng, so-called red ginseng) also exhibited the inhibitory effect at high concentration (500 μg and 100 μg/ml). On the other hand, the remarkable inhibitory effects were not seen in either *Panax japonica* nor *Panax ginseng* (white ginseng). On the bases of these results, the details of the anti-tumor-promoting activity of *P. notoginseng* and its con- stituents were investigated for their cancer chemopreventive activity.

P. notoginseng is distributed in limited parts of China, Yunnan and Kweichow, and is recently cultivated in Yunnan, China. The root of this plant, called Sanchi-Ginseng, is famous Chinese medicine used mainly as a hemostatic drug and the treatment of hepatitis differently from the medicinal use of white- or red-ginseng.

vesicles at any given time. Also note that a small number of vesicle trafficking molecules may populate any given vesicle, precluding their detection by immunofluorescence.

Recombinant Expression of Epitope-Tagged Membrin and msec22b Disrupts Trafficking to the Golgi

Proteins expected to require ER-to-Golgi transport to maintain their localizations include resident Golgi membrane proteins, cargo proteins, and the vesicle trafficking proteins themselves. Our results indicate that at least one of these classes, the vesicle trafficking proteins, was dramatically affected by *myc*-membrin and *myc*-msec22b expression. It was somewhat surprising that syntaxin 5, normally assumed to reside statically in the Golgi, was so dramatically affected by the imbalance of ER-to-Golgi vesicle trafficking proteins. These results imply that even apparently static vesicle trafficking proteins are more dynamic than originally envisioned. It is not known if generic Golgi resident proteins, such as enzymes, depend so heavily upon vesicle-mediated ER-to-Golgi transport to maintain their steady-state positions in the Golgi. Future studies analyzing the kinetics of transport of cargo proteins will be required to determine if the observed trafficking phenotype penetrates to cargo protein transport as well. However, it is extremely likely that it does, since cargo protein transport is dramatically affected by other perturbations of syntaxin 5 expression/localization (Dascher et al., 1994).

It was not unexpected that recombinant expression of full-length membrin and msec22b constructs, as opposed to purposively created mutants, caused a trafficking defect. In a study on cargo protein transport, recombinant expression of epitope-tagged full-length syntaxin 5 caused a specific trafficking defect, while syntaxin 5 lacking its transmembrane region had a less potent effect (Dascher et al., 1994). We reason that production of the trafficking defect may require a relatively higher concentration of the recombinant protein on the membrane than is produced in cells expressing the deleted proteins. In addition, the topological constraints of insertion in a lipid bilayer may be required to produce the functional imbalance.

Vesicle-Trafficking Intermediate(s) in ER/Golgi Transport

The complexes characterized here are likely to represent the functional homologs of the 7 S and 20 S complexes characterized previously from the synapse (Söllner et al., 1993b). These synaptic complexes have been interpreted to be sequential intermediates along a reaction pathway; however, to date the order of occurrence of the intermediates and their functional consequences have not been resolved. For example, the impact of NSF on vesicle trafficking protein interactions has recently been reinterpreted to involve a priming (Banerjee et al., 1996) or predocking (Mayer et al., 1996) step, rather than to follow docking as a late event preceding membrane fusion as originally proposed (Söllner et al., 1993b). The ability of NSF to dissociate both the synaptic and the ER/Golgi trafficking complexes, however, supports the hypothesis that at least in vitro NSF mediates a similar late-stage rearrangement of docking interactions between proteins of the donor and acceptor compartments at all or many steps of the secretory pathway. It remains possible that specific trafficking steps may require NSF for distinct purposes. Perhaps NSF is a protein trafficking chaperone with actions at multiple stages of the biochemical pathway leading to vesicle docking and membrane fusion.

The oligomeric particle characterized in this study is not a homogeneous population and contains at least two separate subcomplexes. We hypothesize that several subcomplexes are likely to be formed from the set of proteins characterized herein. In one type of subcomplex, syntaxin 5 may be separately associated with rsly1 in the absence of the smaller type II membrane proteins. This would coincide with the notion from the synapse that the sec1p family of proteins binds to syntaxins to regulate their activity/availability for engaging in docking interactions (Pevsner et al., 1994).

But why does the ER-to-Golgi trafficking step involve at least 5 type II membrane proteins, when 3 proteins appear to be sufficient in the synapse and for Golgi-to-plasma membrane trafficking in yeast? Mutually exclusive subsets of protein–protein interactions, as elucidated in Figure 8, may represent a key feature of such complexities as the trafficking of multiple distinct vesicle types. If several functionally distinct vesicle types exist for anterograde ER-to-Golgi traffic, each may shuttle different sets of cargo molecules, display distinct or partially distinct sets of v-SNAREs on their surface, and/or be competent to dock and fuse with distinct t-SNARE complexes containing syntaxin 5 in association with different proteins. One hypothesis consistent with our data would involve distinct vesicle types docking to either syntaxin 5–rbet1 or syntaxin 5–GOS-28, depending on the conformation of membrin, rsec22b, and other protein(s) actively displayed on their surface.

In contrast, the large number of type II membrane proteins and independent subcomplexes may provide the framework of an apparatus for regulating anterograde and retrograde transport of vesicles. Regulated protein–protein interactions among two or more v-SNAREs could determine whether a vesicle is competent to dock and fuse with either a *cis*-Golgi syntaxin 5-containing t-SNARE complex or an ER t-SNARE apparatus containing at least one as-yet-undiscovered protein. The precise manner in which combinatorial subsets of v- and t-SNAREs specify anterograde and retrograde docking awaits future experiments. Such a mechanism, however, is inherently feasible, since rab proteins have been demonstrated to regulate associations among SNAREs on vesicles (Lian et al., 1994). A combinatorial model has the appeal of specifying both directions of travel while utilizing one small set of cycling vesicle proteins.

Now that a set of mammalian proteins sufficient to explain aspects of docking and/or fusion between the ER and the Golgi has been established, critical tests of the hypotheses put forth above should proceed rapidly. Furthermore, several homologs of VAMP and syntaxin can be found in the expressed sequence tag (EST) databases. As shown here and in the synapse, donor and

acceptor compartment proteins pair when cells are solubilized in detergent. Therefore, it should now be possible to use the EST database in conjunction with immunoprecipitation experiments to completely characterize the set of proteins responsible for the membrane organization of cells.

Experimental Procedures

Antisera

Anti-syntaxin 5, -syntaxin 6, -*myc*, and -calnexin antisera were described previously (Bock et al., 1996; Hay et al., 1996). A GOS-28 monoclonal antibody (HFD9) was a gift from Drs. W. Hong and V. N. Subramaniam. Rabbit anti-rbet1 and mouse anti-msec22b antisera were prepared by immunizations with bacterially expressed histidine-tagged protein (amino acids 2–95 and 2–195, respectively). Anti-syntaxin 5 and -rbet1 antisera were affinity purified using bead-immobilized antigen and were specific for their respective antigens, recognizing only the corresponding protein bands in immunoblotting experiments with rat liver salt-stripped membranes (data not shown). All immunoblotting experiments utilized ECL (Amersham).

Immunoprecipitation Experiments and Glycerol Velocity Gradients

Affinity-purified anti-syntaxin 5, anti-rbet1 antibodies, and control antibodies were bound to protein A–Sepharose and cross-linked with dimethylpimedilate (DMP). Fresh livers from Sprague Dawley rats were homogenized in homogenization buffer (same as in Hay et al., 1996, but in addition containing 5.75 mM diisopropyl fluorophosphate [DFP], 2 μg/ml leupeptin, 4 μg/ml aprotinin, 0.7 μg/ml pepstatin) using a Potter Elvejem homogenizer. Homogenate was centrifuged at 1000 × g for 15 min, and the resulting supernatant was centrifuged at 107,000 × g for 1 hr. The membrane pellet was then rehomogenized in KCl buffer (20 mM HEPES [pH 7.2], 1 M KCl, 2 mM EGTA, 2 mM EDTA, 1 mM DTT, plus the above protease inhibitors) and incubated for 45 min with agitation. A final 107,000 × g centrifugation was performed, the supernatant discarded, and the pellet rehomogenized in immunoprecipitation buffer (same as KCl buffer but containing 100 mM KCl) and adjusted to a protein concentration of 5 mg/ml. This fraction was extracted with 1% Triton X-100, followed by centrifugation at 107,000 × g for 1 hr. The supernatant was preadsorbed with protein A–Sepharose and then mixed with antibody beads with agitation for 2 hr at 4°C. Following the binding step, beads were centrifuged for 2 min at 2000 × g, and the supernatant removed and saved. Beads were then washed rapidly 4 times with immunoprecipitation buffer containing 1% (first 3 washes) and 0.2% (final wash) Triton X-100. For small-scale experiments (e.g., Figure 1B), washed beads were resuspended directly in one-tenth the volume of original extract in SDS sample buffer. For large-scale experiments (e.g., Figure 2) washed beads from multiple immunoprecipitation reactions were eluted with 0.1M glycine (pH 2.5), neutralized with Tris, and concentrated prior to electrophoresis. Glycerol gradients in immunoprecipitation buffer and 0.2% Triton X-100 were prepared as described (Ting et al., 1995). Samples were either control membrane extracts (see above) or extracts preincubated for 30 min with 240 μg/ml each of histidine-tagged NSF and histidine-tagged α-SNAP (Söllner et al., 1993a), and either 500 μM ATPγS or 500 μM ATP with 8 mM magnesium chloride.

Protein Sequencing

To sequence the proteins shown in Figure 2, eluted proteins collected from 288 ml of membrane extract (1.44 g of membrane protein) were pooled and electrophoresed on SDS gels, followed by transfer to nitrocellulose. Digestion with trypsin, HPLC purification of peptides, and Edman microsequencing were carried out by Drs. W. Lane and J. Neveu at the Harvard Microchemistry Facility.

cDNA Cloning and Sequence Analysis

I.M.A.G.E. Consortium CloneID 455902 (Lennon et al., 1996) from a mouse placenta cDNA library appeared to encode the 23 kDa protein (msec22b) and was obtained from American Type Culture Collection (Rockville, MD). The first amino acid of this protein was assigned to be the first methionine following an in-frame stop codon. GenBank and EMBL database searches (see Hay et al., 1996, for methods) revealed that msec22b was more similar to rsec22a (Hay et al., 1996) and yeast Sec22p than to any other proteins in the database. I.M.A.G.E. clone 390902, from a mouse whole-embryo cDNA library, appeared to encode part of the 25 kDa protein (membrin) and was obtained from Research Genetics Inc. (Huntsville, AL). A PCR probe generated using this clone as a template was utilized to screen adult rat liver and brain cDNA libraries (see Hay et al., 1996, for libraries and methods). The protein coding sequences of full-length brain and liver clones were found to be identical. The first amino acid was the first methionine following an in-frame stop codon. GenBank and EMBL database searches revealed that membrin was strikingly similar to a hypothetical 24.7 kDa protein (BO272.2) from C. elegans chromosome III (GenBank accession number Z46240); no other sequences retrieved in the search appeared to be meaningful.

The multiple sequence alignments displayed in Figures 3 and 4 were obtained using the PILEUP program (Genetics Computer Group). Separate pairwise alignments were also performed using the BESTFIT program to judge the statistical significance of the similarities (see Hay et al., 1996). Percent identities and *z* numbers for each of the pairwise alignments are as follows: rsec22a versus msec22b, 35%, 16.9; rsec22a versus yeast Sec22p, 32%, 14.4; msec22b versus yeast Sec22p, 38%, 24.9; membrin versus BO272.2, 34%, 23.5; membrin versus yeast Bos1p, 22%, 8.2; BO272.2 versus yeast Bos1p, 25%, 7.0. *z* numbers near 1 are expected for unrelated sequences, whereas 10 or higher is considered likely to reflect an evolutionarily significant relationship.

Expression Constructs, Transfections, and Immunofluorescence Microscopy

DNA constructs encoding full-length or membrane anchor-deleted versions of msec22b and membrin were engineered with an amino-terminal *myc* epitope tag and subcloned into the mammalian expression vector pCMV, using our previous methodology (Hay et al., 1996). *myc*-msec22bΔTM was truncated after amino acid 195, *myc*-membrinΔTM after amino acid 190. COS cells were maintained, transfected, and immunostained as described previously (Hay et al., 1996).

Quantification of Trafficking Defect Caused by *myc*-Membrin and *myc*-msec22b Expression

The observer categorized the endogenous syntaxin 5 staining in >150 COS cells per condition regardless of the intensity and staining pattern of the recombinant expressed protein. Syntaxin 5 staining was categorized as either the typical tight juxtanuclear pattern resembling the Golgi indicated by an arrowhead in Figure 6B, a tight juxtanuclear staining pattern significantly fainter than in surrounding cells (not pictured in Figure 6), or an atypical pattern where no outline of a tight juxtanuclear structure was visible, as in the arrowheaded cells in Figures 6D and 6F. For nontransfected COS cells, 83.2%, 3.6%, and 13.2% of cells examined fell into the above categories, respectively. The corresponding percentages for COS cells transfected with the *myc*-tagged constructs were as follows: *myc*-rsec22a, 75.2%, 6.4%, 18.4%; *myc*-membrin, 13.7%, 20.5%, 65.8%; *myc*-membrinΔTM, 75.2%, 12.4%, 12.4%; *myc*-msec22b, 30.1%, 17%, 52.8%; *myc*-membrinΔTM, 76.4%, 12.4%, 9.2%. The quantitation was repeated with the same categories using endogenous rbet1 Golgi staining in place of syntaxin 5, producing qualitatively and quantitatively similar results.

Acknowledgments

We thank Drs. Wanjin Hong and V. Nathan Subramanian for providing anti-GOS-28 antibodies.

Received January 10, 1997; revised February 24, 1997.

References

Banerjee, A., Barry, V.A., DasGupta, B.R., and Martin, T.F.J. (1996). N-ethylmaleimide-sensitive factor acts at a prefusion ATP-dependent step in Ca^{2+}-activated exocytosis. J. Biol. Chem. *271*, 20223–20226.

Table 3. Percentages of EBV-EA Induction in Presence of Extracts of *Panax* Plants with Respect to Positive Control (100%)

Sample	Concentration (μg/ml)[1]			
	500	100	50	10
Panax notoginseng	0.0[2] (60)[3]	7.6 (70)	33.4 (>80)	53.8 (>80)
Panax ginseng (white)	38.7 (70)	79.6 (>80)	100.0 (>80)	100.0 (>80)
Panax ginseng (red)	13.5 (60)	22.4 (>80)	75.3 (>80)	100.0 (>80)
Panax japonica	83.2 (50)	100.0 (>80)	100.0 (>80)	100.0 (>80)

[1] μg/ml, TPA (20 ng = 32 pmol).
[2] Values represent percentages relative to the positive control.
[3] Values in parentheses are viability percentages of Raji cells.

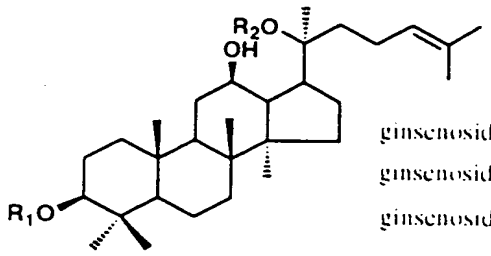

	R_1	R_2
ginsenoside-Rb_1 :	-Glc[2]-Glc	-Glc[6]-Glc
ginsenoside-Rb_2 :	-Glc[2]-Glc	-Glc[6]-Ara(p)
ginsenoside-Rd :	-Glc[2]-Glc	-Glc

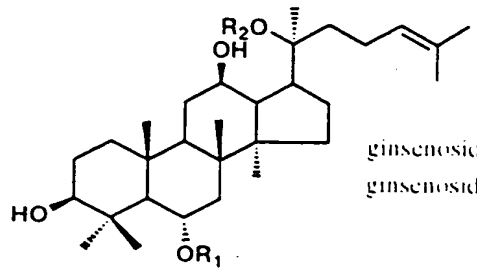

	R_1	R_2
ginsenoside-Re :	-Glc[2]-Rham	-Glc
ginsenoside Rg_1 :	-Glc	-Glc

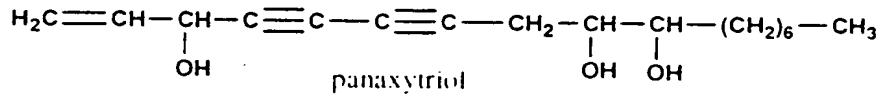

panaxytriol

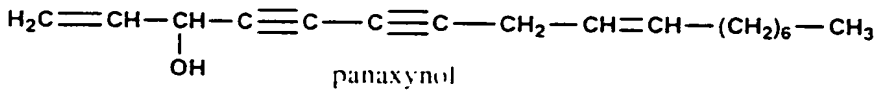

panaxynol

Chart 3. Saponins and Acetylenes from Panax notoginseng

Five dammaranesaponins (ginsenoside-Rb_1, -Rb_2, -Rd, -Re and Rg_1) have been isolated as major neutral saponins from the root of *P. notoginseng* together with other minor saponins.[7] Furtheremore, an acetylene derivative, panaxytriol, which had been obtained from red ginseng, but not from white ginseng,was also isolated and identified. These five saponins and acetylenes were assayed on EBV-EA activation, and these results were shown in Table 4. Of these compounds, acetylenes showed significant inhibitory effects (more than 80% inhibition of activation at 1 x 10 mol ratio/TPA), but they have very strong cytotoxicities on Raji cells (0% viability of Raji cells at 1 x 10^2 mol ratio/TPA, and less than 30% viability of them at 5 x 10 mol ratio/ TPA). On the other hand, ginsnoside- Rg_1 exhibited most strong inhibitory effects (100% inhibition of activation at 2.5 x 10^3 mol ratio/TPA, and more than 85%, 65% and 35% inhibition at 1 x 10^3, 5 x 10^2, and 1 x10^2 mol ratio/TPA) in these five saponins and preserved the high viability even at high concentration.

Table 4. Percentages of EBV-EA Induction in Presence of Ginsenosides and Acetylenes with Respect to Positive Control (100%)

Sample	Concentration (mol ratio, compound/TPA)				
	2.5×10^{3}	1×10^{3}	5×10^{2}	1×10^{2}	1×10
ginsenoside Rb_1	0.0[1] (>80)[2]	20.1 (>80)	41.7 (>80)	71.8 (>80)	100.0 (>80)
ginsenoside Rb_2	0.0 (>80)	22.6 (>80)	48.3 (>80)	78.5 (>80)	100.0 (>80)
ginsenoside Rd	0.0 (>80)	17.6 (>80)	38.0 (>80)	67.4 (>80)	94.8 (>80)
ginsenoside Re	0.0 (>80)	18.9 (>80)	40.7 (>80)	69.3 (>80)	94.4 (>80)
ginsenoside Rg_1	0.0 (>80)	12.4 (>80)	32.5 (>80)	63.6 (>80)	91.0 (>80)
	Concentration (mol rtio, compound/TPA)				
	1×10	1×10^{2}	5×10	1×10	x 1
panaxytriol	---[3] (0)	--- (0)	--- (0)	0.0 (20)	64.9 (>80)
panaxynol	--- (0)	--- (0)	0.0 (30)	23.3 (60)	84.5 (60)

[1] Values represent percentages relative to the positive control value (100%).
[2] Values in parentheses are viability percentage of Raji cells. [3] not detected.

Further, Professor O. Tanaka and his coworkers have reported analysis of saponins of ginseng, and it was clear that the content of ginsenoside-Rg_1 in the root of *P. noto- ginseng* was more than 10 times in other *Panax* plants.[10] In view of this fact, it was deduced that ginsenoside-Rg_1 had the inhibitory effects on EBV-EA activation in itself and, in addition, strongly enhanced the inhibitory effect of panaxytriol. Therefore, it was deduced that the significant inhibitory activity of the crude extract of *P. notoginseng* is exhibited by the combination of ginsenoside-Rg_1 with panaxytriol. The inhibitory effects of ginsenoside-Rg_1 and the crude extracts of *P. notoginseng* on two-stage carcinogenesis test *in vivo* were investigated as follows.

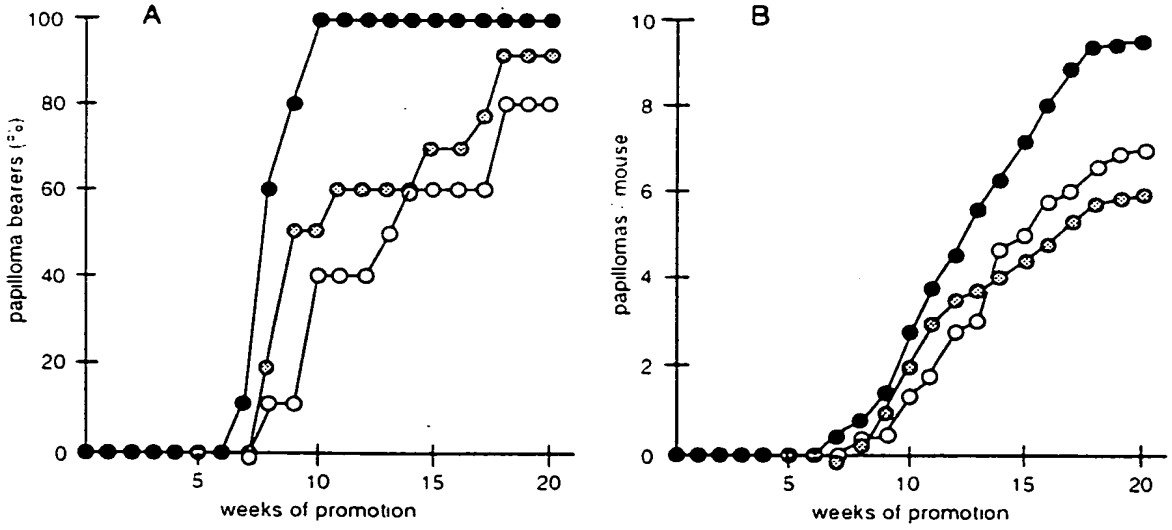

Figure 5. Inhibition of TPA-Induced Tumor Promotion by Multiple Application of ginsenoside-Rg_1 and glycyrrhetic acid.
Treatments of all mice were initiated with DMBA (100 μg, 394 nmol) and promoted with TPA (1 μg, 1.7 nmol) given twice weekly starting 1 week after initiation.
A: Percentages of mice with papillomas. B: Average number of papillomas per mouse.
●, control TPA alone; ○, TPA + 85 nmol of ginsenoside-Rg_1; ⊗, TPA + 85 nmol of glycyrrhetic acid.

Bennett, M.K., and Scheller, R.H. (1993). The molecular machinery for secretion is conserved from yeast to neurons. Proc. Natl. Acad. Sci. USA *90*, 2559–2563.

Bennett, M.K., García-Arrarás, J.E., Elferink, L.A., Peterson, K., Fleming, A.M., Hazuka, C.D., and Scheller, R.H. (1993). The syntaxin family of vesicular transport receptors. Cell *74*, 863–873.

Bloom, G.S., and Brashear, T.A. (1989). A novel 58 kDa protein associates with the Golgi apparatus and microtubules. J. Biol. Chem. *264*, 16083–16092.

Bock, J.B., Lin, R.C., and Scheller, R.H. (1996). A new syntaxin family member implicated in targeting of intracellular transport vesicles. J. Biol. Chem. *271*, 17961–17965.

Dascher, C., and Balch, W.E. (1996). Mammalian Sly1 regulates syntaxin 5 function in endoplasmic reticulum to Golgi transport. J. Biol. Chem. *271*, 15866–15869.

Dascher, C., Ossig, R., Gallwitz, D., and Schmitt, H.D. (1991). Identification and structure of four yeast genes (*SLY*) that are able to suppress the functional loss of *YPT1*, a member of the RAS superfamily. Mol. Cell. Biol. *11*, 872–885.

Dascher, C., Metteson, J., and Balch, W.E. (1994). Syntaxin 5 regulates endoplasmic reticulum to Golgi transport. J. Biol. Chem. *269*, 29363–29366.

Hardwick, K.G., and Pelham, H.R.B. (1992). *SED5* encodes a 39-kD integral membrane protein required for vesicular transport between the ER and Golgi complex. J. Cell Biol. *119*, 513–521.

Hay, J.C., Hirling, H., and Scheller, R.H. (1996). Mammalian vesicle trafficking proteins of the endoplasmic reticulum and Golgi apparatus. J. Biol. Chem. *271*, 5671–5679.

Lawton, M.P., Gasser, R., Tynes, R.E., Hodgson, E., and Philpot, R.M. (1990). The flavin-containing monooxygenase enzymes expressed in rabbit liver and lung are products of related but distinctly different genes. J. Biol. Chem. *265*, 5855–5861.

Lennon, G.G., Auffray, C., Polymeropoulos, M., and Soares, M.B. (1996). The I.M.A.G.E. consortium: an integrated molecular analysis of genomes and their expression. Genomics *33*, 151–152.

Lian, J.P., and Ferro-Novick, S. (1993). Bos1p, an integral membrane protein of the endoplasmic reticulum to Golgi transport vesicles, is required for their fusion competence. Cell *73*, 735–745.

Lian, J.P., Stone, S., Jiang, Y., Lyons, P., and Ferro-Novick, S. (1994). Ypt1p implicated in v-SNARE activation. Nature *372*, 698–701.

Mayer, A., Wickner, W., and Haas, A. (1996). Sec18p (NSF)-driven release of Sec17p (α-SNAP) can precede docking and fusion of yeast vacuoles. Cell *85*, 83–94.

Nagahama, M., Orci, L., Ravazzola, M., Amherdt, M., Lacomis, L., Tempst, P., Rothman, J.E., and Söllner, T.H. (1996). A v-SNARE implicated in intra-Golgi transport. J. Cell Biol. *133*, 507–516.

Newman, A.P., Groesch, M., and Ferro-Novick, S. (1992). Bos1p, a membrane protein required for ER to Golgi transport in yeast, copurifies with the carrier vesicles and with Bet1p and the ER membrane. EMBO J. *12*, 3609–3617.

Peterson, M.R., Hsu, S.-C., and Scheller, R.H. (1996). A mammalian homologue of *SLY1*, a yeast gene required for transport from the endoplasmic reticulum to Golgi. Gene *169*, 293–294.

Pevsner, J., Hsu, S.-C., Braun, J.E.A., Calakos, N., Ting, A.E., Bennett, M.K., and Scheller, R.H. (1994). Specificity and regulation of a synaptic vesicle docking complex. Neuron *13*, 353–361.

Rexach, M.F., Latterich, M., and Schekman, R.W. (1994). Characteristics of endoplasmic reticulum-derived transport vesicles. J. Cell Biol. *126*, 1133–1148.

Shim, J., Newman, A.P., and Ferro-Novick, S. (1991). The *BOS1* gene encodes an essential 27-kD membrane protein that is required for vesicular transport from the ER to the Golgi complex in yeast. J. Cell Biol. *113*, 55–64.

Søgaard, M., Tani, K., Ye, R.R., Geromanos, S., Tempst, P., Kirchhausen, T., Rothman, J.E., and Söllner, T. (1994). A rab protein is required for the assembly of SNARE complexes in the docking of transport vesicles. Cell *78*, 937–948.

Söllner, T., Whiteheart, S.W., Brunner, M., Erdjument-Bromage, H., Geromanos, S., Tempst, P., and Rothman, J.E. (1993a). SNAP receptors implicated in vesicle targeting and fusion. Nature *362*, 318–324.

Söllner, T., Bennett, M.K., Whiteheart, S.W., Scheller, R.H., and Rothman, J.E. (1993b). A protein assembly-disassembly pathway in vitro that may correspond to sequential steps of synaptic vesicle docking, activation, and fusion. Cell *75*, 409–418.

Subramaniam, V.N., Peter, F., Philp, R., Wong, S.H., and Hong, W. (1996). GS28, a 28-kilodalton Golgi SNARE that participates in ER-Golgi transport. Science *272*, 1161–1163.

Ting, A.E., Hazuka, C.D., Hsu, S.-C., Kirk, M.D., Bean, A.J., and Scheller, R.H. (1995). rsec6 and rsec8, mammalian homologs of yeast proteins essential for secretion. Proc. Natl. Acad. Sci. USA *92*, 9613–9617.

GenBank Accession Numbers

The GenBank accession number for the mouse sec22b (msec22b) sequence is U91538. The GenBank accession number for the rat membrin sequence is U91539.

Erratum

J. L. Kim, K. A. Morgenstern, C. Lin, T. Fox, M. D. Dwyer,
J. A. Landro, S. P. Chambers, W. Markland, C. A. Lepre,
E. T. O'Malley, S. L. Harbeson, C. M. Rice, M. A. Murcko,
P. R. Caron, and J. A. Thomson

In our paper entitled "Crystal Structure of the Hepatitis C Virus NS3 Protease Domain Complexed with a Synthetic NS4A Cofactor Peptide" (1996, Cell *87*, 343–355), we reported the amino acid sequence of the HCV NS3 protease domain used for the study with a single residue error in Figure 5. Residue 1190 was incorrectly labeled as "T" (threonine). The correct residue at position 1190 in the HCV NS3 sequence used is "A" (alanine). We sincerely regret any inconvenience this has caused; however, all interpretations and conclusions of the work remain as originally stated.

In the positive control, more than 80% and 100% of mice bore papillomas at 9 and 10 weeks of promotion, respectively, as shown in Fig. 5A. Further, more than 10 papillomas were formed per mouse at 20 weeks of promotion, as shown in Fig. 5B. On the other hand, when ginsenoside-Rg_1 was applied continuously before each TPA treatment, it remarkably delayed the formation of papillomas in mouse skin and reduced the number of papillomas per mouse (only about 10% and 30% of mice bore papillomas at 9 and 12 weeks of promotion, respectively, 80% of mice bore papillomas even at 20 weeks, and less than 8 papillomas were formed per mouse at 20 weeks of promotion. In our experiments, these inhibitory effects of ginsenoside-Rg_1 are similar to those of glycyrrhetic acid which has been known as a strong antitumor promoter.

And, in our laboratory, it was also found that the ginsenoside-Rg_1 enhanced the weak inhibitory effects of *P. ginseng* (white-ginseng), when -Rg1 was additionaly applied with the extract of white ginseng. Further, -Rg_1 also showed inhibitory effects by oral administration on mouse skin carcinogenesis promoted by ultaviolet (UVB) irradiation.[11]

Antitumor promoting Effects of Extract of *P. notoginseng*

As shown in Fig. 6, the MeOH extract of *P. notoginseng* exhibited strong inhibitory effects. When the extract was continuously applied 1 hr before each TPA treatment (pre-treatment experiments), 50%, 80%, and 90% of mice bore papillomas at 12, 16 and 20 weeks of promotion, respectively, and only 4 and 5 papillomas were formed per mouse at 15 and 20 weeks of promotion, respectively. When this extract was applied 0.5 hr after each TPA treatment (post-treatment experiments), its inhibitory effects (only 20%, 50% and 70% of mice bore papillomas at 11, 15 and 20 weeks of promotion, and less than 1, 2 and 3 papillomas were formed per mouse at 10, 15 and even at 20 weeks of promotion, respectively)were stronger than the case of pre-treatment experiments.

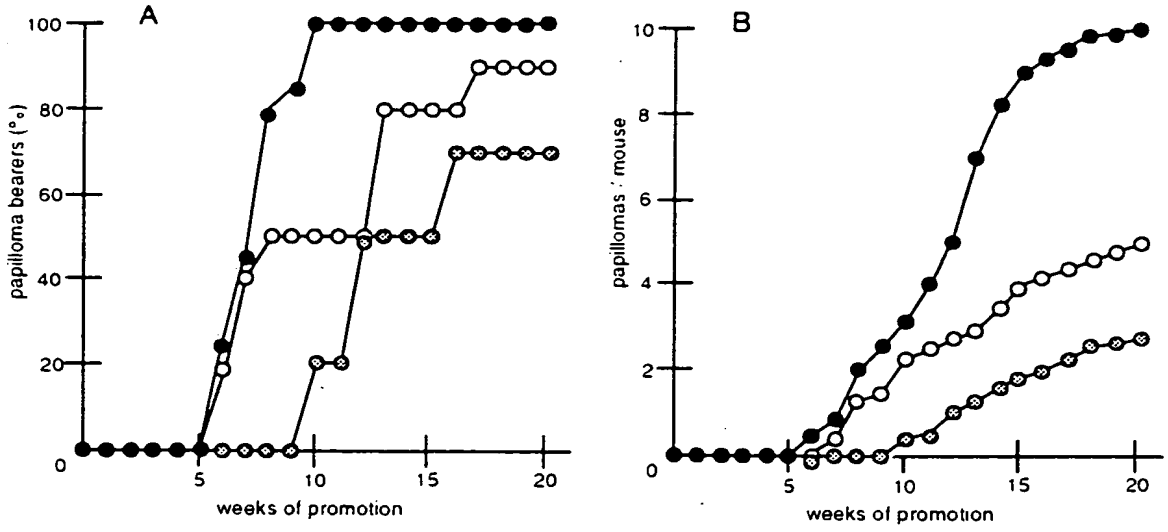

Figure 6. Inhibition of TPA-Induced Tumor Promotion by Multiple Application of MeOH extract of *P. notoginseng*.
Treatments of all mice were initiated with DMBA (100 μg, 394 nmol) and promoted with TPA (1 μg, 1.7 nmol) given twice weekly starting 1 week after initiation.
A: Percentages of mice with papillomas. B: Average number of papillomas per mouse.
●, control TPA alone; ○, TPA + treated with 50 mg of MeOH extract of *P. notoginseng* 1 hr before each TPA treatment (pre-treatment); ⊛, TPA + treated with 50 mg of MeOH extract of *P. notoginseng* 0.5 hr after each TPA treatment (post-treatment).

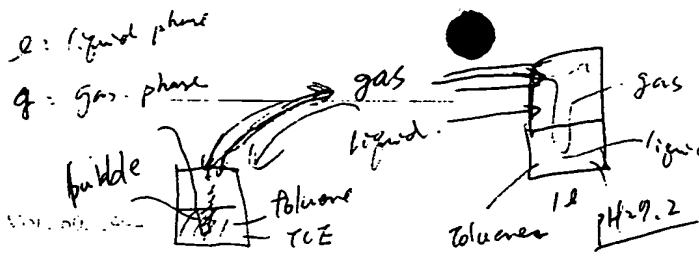

concentration (micromolar); $C_{L,X}$, biomass concentration in the liquid phase (milligrams per liter); C_i, liquid-phase concentration at gas-liquid interface (micromolar); ϕ_G, volumetric gas flow rate (liters per minute); ϕ_L, volumetric liquid flow rate (liters per minute); k_L, liquid side mass-transfer coefficient (meters per minute); $K_{i,C}$, toluene inhibition constant of TCE degradation (micromolar); $K_{i,S}$, TCE inhibition constant of toluene degradation (micromolar); K_s, Michaelis-Menten half-saturation constant (micromolar); R_s, volumetric conversion rate (micromoles per minute); V_L, liquid volume reactor (working volume; liters); V_{max}, maximum specific conversion rate (micromoles per minute per milligram of cells); $Y_{X/S}$, overall yield coefficient of biomass on substrate (milligrams of cells per micromole). Subscripts denote the following parameters: *X*, biomass; *S*, growth substrate; *C*, cometabolized substrate (TCE).

Bacterial strain and culture conditions. *P. cepacia* G4 (19) was a gift from M. S. Shields, U.S. Environmental Protection Agency, Gulf Breeze, Fla. The organism was grown in a 1-liter fermentor with toluene as the carbon and energy source. The medium contained (per liter) 6.9 g of $Na_2HPO_4 \cdot 12H_2O$, 2.4 g of KH_2PO_4, 1.5 g of $(NH_4)_2SO_4$, 0.2 g of $MgSO_4 \cdot 7H_2O$, 30 mg of yeast extract (BBL Laboratories), and 5 ml of a trace elements solution (15). Prior to sterilization, the medium was acidified with concentrated H_2SO_4 to a pH of 2 to 3. The pH in the fermentor was regulated at 7.2 with 2 N KOH. Toluene and TCE were supplied by bubbling a filtered (ACRO 50; Gelman) air-toluene-TCE mixture through the reactor. The feed of toluene was generated by passing a stream of air through a flask containing pure toluene, which was subsequently diluted into the main airflow. Addition of TCE to the continuous culture was accomplished by diluting TCE-saturated air with air containing no TCE and introducing only a fraction of the diluted TCE gas into the main airflow (21). Other conditions were as follows: working volume, 800 ml; temperature, 28°C; impeller speed, 900 rpm; airflow rate, ca. 50 ml/min; dilution rate, 0.083 h^{-1}.

Analytical methods. TCE, toluene, and oxygen were measured by gas chromatography. Concentrations in the gas phase were determined after sampling with a gas-tight syringe (Pressure-Lok, series A-2). TCE and toluene in the gas phase were analyzed with a flame ionization detector. The accuracy (standard deviation) of this method was better than 5%, with a detection limit of approximately 50 nM. Oxygen in the gas phase was analyzed on a Molsieve 5A packed column equipped with a thermal conductivity detector. With a standard deviation of less than 5%, these measurements also had a high precision. Concentrations of TCE and toluene in the liquid phase were measured with pentane-extracted samples (31). Samples (4.5 ml) were extracted with 1.5 ml of pentane containing 0.05 mM 1-bromohexane as an internal standard. Gas chromatography conditions were as described previously (24). An electron capture detector was used for the analysis of TCE, and a flame ionization detector was used for the analysis of toluene in the liquid phase. The determinations of the toluene and TCE concentrations in the liquid phase were much less reproducible than the gas phase measurements; concentration differences of up to 20% between duplicates occurred in all of the nine steady states characterized. Oxygen in the liquid phase was monitored with a probe, as described before (25).

Chloride production was determined with a colorimetric assay (15).

Modeling. A mathematical model was used to describe the simultaneous conversion of TCE and toluene by *P. cepacia* G4 during steady-state growth on toluene. The model was based on the following assumptions: (i) the rate of degradation of TCE and toluene by *P. cepacia* G4 can be described by Michaelis-Menten-type kinetics adapted to include competitive inhibition; (ii) the gas phase and the liquid phase in the chemostat are ideally mixed; (iii) the overall growth yield of the cells on toluene is not affected by the conversion of TCE; and (iv) mass transfer from the gas phase via the aqueous phase to the cells can be described by the film model (32). Mass-transfer resistance is supposed to be located solely in the liquid phase.

The model is based on five equations. For the degradation kinetics, Michaelis-Menten-type equations are used, assuming a competitive inhibition between the substrate (toluene) and contaminant (TCE):

$$R_s = -V_{max,S} \frac{C_{i,S}}{C_{i,S} + K_{m,S}\left(1 + \frac{C_{i,C}}{K_{i,S}}\right)} C_{L,X} \quad (1)$$

$$R_c = -V_{max,C} \frac{C_{i,C}}{C_{i,C} + K_{m,C}\left(1 + \frac{C_{i,S}}{K_{i,C}}\right)} C_{L,X} \quad (2)$$

The symbols used are explained above in the nomenclature section. The constant overall growth yield on the substrate is given by

$$Y_{X/S} = -\frac{R_X}{R_S} \quad (3)$$

Finally, mass balances for both the gas and liquid phases are formulated as follows:

$$\phi_G(C_{G,i} - C_G) - k_L a\,(C_i^* - C_i)\,V_L = 0 \quad (4)$$

$$\phi_L(C_{L,i} - C_L) + k_L a\,(C_i^* - C_i)\,V_L + RV_L = 0 \quad (5)$$

Determination of kinetic parameters. The $k_L a$ values for toluene (1.67 min^{-1}) and TCE (1.75 min^{-1}) were calculated from the $k_L a$ value for oxygen, using the equation described by Westerterp et al. (32). The $k_L a$ value for oxygen (2.61 min^{-1}) was determined by the steady-state oxygen balance method (26).

The kinetic constants $V_{max,S}$ (0.07 μmol/min/mg of cells), $V_{max,C}$ (5.0×10^{-3} μmol/min/mg of cells), $K_{m,C}$ (6 μM), and $K_{m,S}$ (25 μM) were estimated from the work of Paul de Graaf in our laboratory (6), who determined these values with *P. cepacia* G4 growing on toluene in a chemostat at dilution rates of 0.07 and 0.09 h^{-1}. These measurements were done by determining substrate depletion rates in batch incubations (30-ml flasks with 10 ml of medium) containing mineral medium, substrate, and cells freshly collected from the chemostat cultures. The flasks were vigorously shaken in order to constantly maintain a distribution close to equilibrium between the liquid and gas phases. Control experiments with the addition of substrate to the liquid phase only indicated that rapid equilibration indeed occurred (mass-transfer coefficient, $k_L a$, ≥6 min^{-1}). The rate of depletion of toluene and TCE was monitored over a 15-min period by gas chromatographic analysis of headspace samples taken with a syringe through viton septa. Degradation rates in the liquid phase were calculated by using the partition coefficients of toluene and TCE (6, 12). The validity of the applied method was also checked by comparing separate gas and liquid phase measurements.

The inhibition constants (K_i values) for TCE and toluene

On the basis of these results, the MeOH extract of *P. notoginseng* might be valuable as an antitumor promoter in chemical carcinogenesis, and the inhibitory effects by oral administration on other forms of carcinogenesis were also investigated.[11]

The two-stage carcinogenesis test of this extract on pulmonary tumor (4-nitroquinoline-*N*-oxide is as an initiator and glycerol is as a promoter) and on liver carcinoma (*N*-nitrosodiethylamine is as an initiator and phenobarbital is as a promoter) were examined.

As shown in Table 5, both the total number of tumors in 15 mice and percentage of mice with pulmonary tumors were remarkably reduced (the number of tumors per mouse is reduced to about one fifth, and more than 40% reduction on the percentages of mice with tumor after 25 weeks) by taking the MeOH extract of *P. notoginseng* together with the promoter (group V) compared with the positive control group (group IV).

Table 5. Incidences of Pulmonary Tumors in Mice Treated with the MeOH Extract of *Panax notoginseng*

Group	Treatment	total No. of tumors	No. of tumor per mouse	% of mice with tumor
I.	water alone [1]	0	0	0
II.	8% glycerol alone [2]	0	0	0
III.	4NQO + water [3]	1	0.06	6.7
IV.	4NQO + 8% glycerol [4]	45	3.0	100
V.	4NQO + 8% glycerol + ext of *P. notoginseng* (1.0 mg/100 ml) [5]	10	0.67	53.3

[1] Without initiation, drinking water alone. [2] Without initiation and 8% glycerol solution has been drunk as the promotion treatment instead of drinking water. [3] Initiated with 4-nitroquinoline-*N*-oxide (4NQO, 0.3 mg/mouse, subcutaneous injection), and drinking water. [4] Initiated with 4NQO, and 8% glycerol solution has been drunk (for 25 weeks) as the promotion treatment instead of drinking water. [5] Initiated with 4NQO, and 8% glycerol solution including the extract of *P. notoginseng* has been drunk (for 25 weeks) as the promotion treatment instead of drinking water.

Table 6. Incidences of Hyperplasia of Liver in Mice Treated with the MeOH Extract of *Panax notoginseng*

Group	Treatment	total No. of hyperplastic nodules	No. of hyperplastic nodules per mouse	% of mice with hyperplastic nodules (%)
I.	water alone [1]	0	0	0
II.	0.09% PB alone [2]	0	0	0
III.	DEN + water [3]	0	0	0
IV.	DEN + 0.09% PB [4]	47	3.13	100
V.	DEN + 0.09% PB + ext of *P. notoginseng* (2.5 mg/100 ml) [5]	23	1.53	46.6

[1] Without initiation, drinking water alone. [2] Without initiation and 0.09% phenobarbital (PB) solution has been drunk as the promotion treatment instead of drinking water. [3] Initiated with N-nitrosodiethylamine (DEN, 1.8 mg/mouse, peritoneal injection), and drinking water. [4] Initiated with DEN, and 0.09% PB solution has been drunk as the promotion treatment instead of drinking water(for 25 weeks). [5] Initiated with DEN, and 0.09% PB solution including the extract of *P. notoginseng* has been drunk as the promotion treatment instead of drinking water (for 25 weeks).

a. (m^2/m^3)

C_g: (μM)

C_{gi}: (μM)

APPLIED AND ENVIRONMENTAL MICROBIOLOGY, Sept. 1994, p. 3368–3374
0099-2240/94/$04.00+0

Vol. 60, No. 9

Cometabolic Degradation of Trichloroethylene by *Pseudomonas cepacia* G4 in a Chemostat with Toluene as the Primary Substrate

ANDREW S. LANDA,[1] E. MARIJN SIPKEMA,[2] JAN WEIJMA,[2] ANTONIE A. C. M. BEENACKERS,[2] IAN DOLFING,[1†] AND DICK B. JANSSEN[1]*

Department of Biochemistry[1] and Department of Chemical Engineering,[2] University of Groningen, Nijenborgh 4, NL-9747 AG Groningen, The Netherlands

Received 21 April 1994/Accepted 30 June 1994

***Pseudomonas cepacia* G4 is capable of cometabolic degradation of trichloroethylene (TCE) if the organism is grown on certain aromatic compounds. To obtain more insight into the kinetics of TCE degradation and the effect of TCE transformation products, we have investigated the simultaneous conversion of toluene and TCE in steady-state continuous culture. The organism was grown in a chemostat with toluene as the carbon and energy source at a range of volumetric TCE loading rates, up to 330 μmol/liter/h. The specific TCE degradation activity of the cells and the volumetric activity increased, but the efficiency of TCE conversion dropped when the TCE loading was elevated from 7 to 330 μmol/liter/h. At TCE loading rates of up to 145 μmol/liter/h, the specific toluene conversion rate and the molar growth yield of the cells were not affected by the presence of TCE. The response of the system to varying TCE loading rates was accurately described by a mathematical model based on Michaelis-Menten kinetics and competitive inhibition. A high load of 3,400 μmol of TCE per liter per h for 12 h caused inhibition of toluene and TCE conversion, but reduction of the TCE load to the original nontoxic level resulted in complete recovery of the system within 2 days. These results show that *P. cepacia* can stably and continuously degrade toluene and TCE simultaneously in a single-reactor system without biomass retention and that the organism is more resistant to high concentrations and shock loadings of TCE than *Methylosinus trichosporium* OB3b.**

Most monohalogenated hydrocarbons can be used as growth substrates by specific microbial cultures, while compounds with two or more halogens per molecule are generally more recalcitrant, especially when the halogens are bound to the same carbon atom (17). The latter compounds, however, are usually biodegradable via cometabolic transformation processes, provided that they have at least one carbon-hydrogen bond. Examples of such compounds are the dichloroethylenes, trichloroethylene (TCE), 1,1-dichloroethane, 1,1,1-trichloroethane, and chloroform (3, 21, 27). Cometabolic conversions of halogenated compounds rely on nonspecific enzymes, usually mono- and dioxygenases that do not specifically cleave carbon-halogen bonds but produce unstable intermediates that release halides by chemical decomposition.

The best-studied compound subject to aerobic cometabolism is TCE. A whole series of organisms have been shown to convert this compound, and attempts have been made to use this knowledge for the development of bioreactor systems for application in various branches of environmental biotechnology. The most critical factors in deciding which organism(s) to take for such bioreactor systems are the specific activity of the cells for TCE and the possible formation of toxic intermediates. On the basis of kinetic criteria, both methanotrophs and toluene oxidizers are suitable candidates (7). In methanotrophs, however, TCE conversion results in inactivation of the cells (1, 2, 5, 13, 23, 29, 30).

Pseudomonas cepacia G4 is the best-known representative of the group of toluene-oxidizing, TCE-degrading bacteria (18–20). The organism has been isolated specifically for its ability to convert TCE. The wild-type strain needs the presence of an aromatic compound such as phenol or toluene for the induction of the TCE-oxidizing enzymes. Kinetic experiments with phenol and TCE have led to the suggestion that the aromatic compound and TCE could be competitive inhibitors (10, 11). This indicates that it may be inefficient to degrade TCE in the presence of an aromatic growth substrate.

The development of a bioreactor system for the continuous degradation of TCE from air with *P. cepacia* G4 as the biocatalyst requires more quantitative data on the kinetic characteristics of the simultaneous conversion of the aromatic growth substrate and TCE and on the possible toxic effects of degradation products of TCE. The stability of the reactor system, which must degrade TCE constantly over a long period, and the ability of the system to withstand varying concentrations of TCE are also important factors. In this paper, we describe the kinetics of simultaneous TCE and toluene degradation in continuous culture. We also present a mathematical model that accurately describes the observed kinetics of TCE and toluene degradation. *P. cepacia* G4 appeared more resistant to high loadings of TCE than the methanotrophic TCE oxidizer *Methylosinus trichosporium* OB3b.

MATERIALS AND METHODS

Nomenclature. The following parameters are used in this paper: a, interfacial area (square meters per cubic meter); C_g, gas phase concentration in the reactor (micromolar); C_{gi}, inlet gas phase concentration (micromolar); C_l, liquid-phase concentration in the reactor (micromolar); C_{li}, inlet liquid-phase

* Corresponding author. Phone: 31-50-634008. Fax: 31-50-634165.
† Present address: Research Institute for Agrobiology and Soil Fertility (AB-DLO), NL-9750 AC Haren, The Netherlands.

Furthermore, the inibitory effects of *P. notoginseng* on liver carcinogenesis are shown in Table 7. In the group of V taking the MeOH extract, the total number of hyperplastic nodules on liver was 23, and the percentages of mice with hyperplastic nodules was less than 50%. On the other hand, in the positive control group (IV group), 47 hyperplastic nodules were formed and 100% of mice had hyperplastic nodules after 25 weeks. Therefore, the MeOH extract of *P. notoginseng* reduced the formation of hyperplastic nodules on the two-stage liver carcinogenesis test. These results of our experiments strongly suggested that *P. notoginseng* is effective as an antitumor promoter on not only the skintumorigenesis but also other carcinogenesis of the internal organs.

CONCLUSION

From the results of our experiments described above, it was concluded that several triterpenoid glycosides and crude drugs containing saponins exhibited antitumor promoting activities on chemical carcinogenesis, and some of them strongly enhanced the inhibitory effects of other constituents. These compounds might be valuable for cancer chemoprevention by natural products. In the case of the hepatitis or the prevention of cancer relapse, we should consider to apply the chemopreventive agents to reduce the severe side actions of anticancer agents. For the application of natural products to chemoprevention, we have many problems to be solved, and one of the most important problem is the inhibitory mechanisms of these compounds on chemical carcinogenesis. Therefore, in many laboratories, the search of new antitumor promoters from natural resources along with the studies of the elucidation of the mechanisms is in progress.

Acknowledgement

I am very grateful to Dr. Harukuni Tokuda of Kyoto Prefectural University of Medicine for biological assays, and to Dr. Mitsumasa Haruna of Meijo University for NMR measurements and helpful discussions. Thanks are also due to Dr. Midori Takasaki of Kyoto Pharmaceutical University for helpful cooperative works and discussions.

REFERENCES

1. I. Berenblum, The mechanism of carcinogenesis, a study of the significance of cocarcinogenic action and related phenomea, *Cancer Res.*, 1: 807 (1941)
2. T. Konoshima, E. Okamoto, M. Kozuka, H. Nishino, H. Tokuda, and M. Tanabe, Studies on inhibitors of skin tumor promotion, III. Inhibitory effects of isoflavonoids from *Wistaria brachybotrys* on Epstein-Barr virus activation, *J. Nat. Prod.*, 51: 1266 (1988); M. Takasaki, T. Konoshima, M. Kozuka, and H. Tokuda, Anti-tumor-promoting activities of euglobals from *Eucalyptus* plants, *Biol. Pharm. Bull.*, 18: 435 (1995).
3. T. Konoshima, M. Takasaki, M. Kozuka, T. Nagao, H. Okabe, N. Irino, T. Nakatsu, H. Tokuda, and H. Nishino, Inhibitory effects of cucurbitane triterpenoids on Epstein-Barr virus activation and two-stage carcinogenesis of skin tumor II., *Biol. Pharm. Bull.*, 18: 284 (1955), and references cited there in.
4. T. Konoshima, M. Kozuka, M. Haruna, and K. Ito, Constituents of Leguminous plants, XIII. New triterpenoid saponins from *Wistaria brachybotrys*, *J. Nat. Prod.*, 54: 830 (1991).
5. I. Kitagawa, M. Yoshikawa, H.K. Wang, M. Saito, V. Tosirisuk, T. Fujiwara, and K. Tomita, Revised structures of soyasapogenol A, B and E, oleanene-sapogenols from soybean. Structures of soyasaponin I, II and III, *Chem. Pharm. Bull.*, 30: 2294 (1982).

6. T. Konoshima, and T. Sawada, Legume saponins of *Gleditsia japonica* Miquel IV, ^{13}C-NMR spectral studies on structure elucidation of saponin B and C, *Chem. Pharm. Bull.*, 30: 2747 (1982), and references cited therein.
7. T. Konoshima, M. Kozuka, T. Sawada, and T. Kimura, Studies on the constituents of Leguminous plants IX. The structure of new triterpenoid saponin from the fruits of *Gymnocladus chinensis* Baillon, *Chem. Pharm Bull.*, 35: 46 (1987), and references cited therein.
8. O. Tanaka and R. Kasai, *Progress in the Chemistry of Organic Natural Products*, W. Herz, H. Grisebach, G.W. Kirby, and Ch. Tamm, Ed. Springer-Verlag, New York (1984); I. Kitagawa, T. Taniyama, T. Hayashi, and M. Yoshikawa, Malonyl ginsenosides Rb_1, Rb_2 and Rd, four new malonylated dammarane-type triterpene glycosides from ginseng radix, *Chem. Pharm. Bull.*, 31: 3353 (1983); S. Sanada, N. Kondo, J. Shoji, O. Tanaka, and S. Shibata, Studies of saponins of ginseng I, structures of ginsenoside-Ro, -Rb_1, -Rb_2, -Rc and -Rd, *Chem. Pharm. Bull.*, 22: 421 (1974).
9. H. Matsuura, R. Kasai, O. Tanaka, Y. Saruwatari, T. Fuwa, and J. Zhou, Further studies on dammarane-saponins of Sanchi-ginseng, *Chem. Pharm. Bull.*, 31: 2281 (1983).
10. H. Yamaguchi, R. Kasai, H. Matsuura, O. Tanaka, and T. Fuwa, High-performance liquid chromatographic analysis of acidic saponins of ginseng and related plants, *Chem. Pharm. Bull.*, 36: 3468 (1988).
11. T. Konoshima, M. Takasaki, H. Tokuda, and H. Nishino, Chemopreventive effects of *Panax notoginseng* on hepatic carcinogenesis, *Proc. 10th Symposium on the Development and Application of Naturally Occurring Drug Materials* (Chiba) p. 45 (1995).

TABLE 4. Values of variables calculated with the mathematical model and compared with those determined experimentally in nine different steady states

Steady state no.	$C_{g,T}$ (μM)		$C_{g,S}$ (μM)		$C_{l,T}$ (mg/liter)		$C_{l,C}$ (μM)		$C_{l,S}$ (μM)	
	Expt	Model	Expt	Model	Expt	Model	Expt	Model	Expt	Model
1	0.0	0.0	1.6	7.2	383	371	0.0	0.0	1.4	16
2	0.2	0.5	1.5	6.6	375	370	0.0	1.1	0.2	15
3	0.8	1.1	4.9	9.6	313	307	0.4	2.3	6.4	24
4	1.4	1.1	5.3	7.4	450	442	0.5	2.4	4.5	16
5	2.4	2.8	5.5	11	350	342	1.0	6.2	4.5	28
6	3.9	4.3	4.8	11	365	353	2.0	9.4	5.2	26
7	13	11	9.4	15	365	359	5.6	23	10	38
8	27	24	14	18	363	356	14	52	9.1	50
9	74	73	52	61	233	218	80	164	126	187

the model were the same as those used in the actual experiments. With this input, it was possible to closely predict the conversion efficiency of both toluene and TCE (Fig. 3). For TCE loading rates of up to 120 μmol/h, the output of the model showed good agreement also with experimentally determined concentrations of toluene and TCE in the gas phase and with the cell density (Table 4). Some fluctuation in the actual amount of biomass can be explained from the measured fluctuations in the toluene feed rate (Table 1). The experimental concentrations of toluene and TCE in the liquid phase did not coincide with the values predicted by the model (Table 4). However, the conversion activities of the cells for TCE and toluene in the fermentor (Table 1) were in accordance with the predicted rates using calculated concentrations in the liquid phase (Table 4).

DISCUSSION

The results indicate that it is possible to cometabolically degrade TCE continuously and stably in a completely mixed system with growing cells. The chemostat was run for more than 6 weeks at various TCE loading rates without toxic effects of TCE or TCE conversion products. The growth yield and the specific activity of the cells for toluene were not affected by TCE loading rates of up to 145 μmol/liter/h. Previous experiments in our laboratory with *M. trichosporium* OB3b in a similar experimental setup (21, 22) showed that the growth yield of the cells on methane decreased with increasing TCE conversion until the system collapsed completely at a TCE loading rate of 13 μmol/liter/h. The highest volumetric activity of the reactor and the highest observed specific activity of the cells were at least 20- and 75-fold higher for *P. cepacia* G4 than for strain OB3b (Table 5). The hypothesis is that the *M. trichosporium* cells get poisoned by conversion products of TCE. Apparently, *P. cepacia* can convert TCE without inactivation of the cells.

P. cepacia G4 also had the capacity to survive temporary high concentrations of TCE. The same was recently found for strain G4 growing in an airlift reactor in the presence of phenol (8). This is important for its potential use in the cleanup of contaminated waste streams in which TCE concentrations can vary considerably.

It is not clear why *M. trichosporium* OB3b is more sensitive to TCE conversion than *P. cepacia* G4. TCE epoxide, the first intermediate in the TCE degradation route of *M. trichosporium* OB3b, can covalently bind to various nucleophilic sites on biological macromolecules (14, 23). Alternatively, the epoxide may decompose to acyl halides, which are extremely reactive and toxic (14). Conceivably, *P. cepacia* is more resistant to TCE, either because less reactive products are formed in this organism or because the organism is less sensitive to the damage caused by TCE degradation products.

The specific TCE degradation rate of *P. cepacia* in the chemostat increased with increasing TCE concentrations according to Michaelis-Menten kinetics, even though the increased TCE concentrations were accompanied by increased toluene concentrations in the liquid phase. The maximally observed specific TCE conversion activity of the cells in the chemostat was 1.6 nmol/min/mg of cells, almost twofold lower than the activity of cells grown on an aromatic substrate and tested for TCE conversion in the absence of this substrate (6, 11). The maximal TCE conversion activities in the reactor were reached at toluene concentrations in the liquid phase of 40 to 150 μM, although at these toluene concentrations inhibition of TCE conversion already occurred.

Our mathematical model for the cometabolic conversion of TCE in the presence of toluene as the growth substrate describes the conversion efficiency of both compounds at the different steady states quite well. The strength of the model is that it is based on some generally accepted principles and, more importantly, needs as input variables only the ingoing flows and concentrations of toluene and TCE.

Usually it is assumed that $K_{i,S}$ (the inhibition constant of TCE on toluene conversion) is equal to $K_{m,C}$ (the Michaelis-Menten half-saturation constant for TCE conversion), while $K_{i,C}$ is equal to $K_{m,S}$ (4). Our data indicate that this is not the case with simultaneous toluene and TCE conversion. This may

TABLE 5. Comparison of TCE transformation characteristics of *P. cepacia* G4 and *M. trichosporium* OB3b in continuous culture

Characteristic	*P. cepacia*	*M. trichosporium*[a]
Growth substrate	Toluene	Methane
Biomass concn (g/liter)	0.4	2.5
Toxicity of TCE transformation	Not observed	Yes
Conversion ratios (μmol of TCE/mmol of growth substrate)	10–50	0.008–0.4
TCE loading rates (μmol/liter/h)		
Stable	7–330	0.08–2.3
Not stable[b]	Not observed	13
$C_{g,C}$ (μM)		
Stable	2–80	0.02–0.6
Not stable[b]	Not observed	3.1
Highest sp act for TCE (nmol/min/mg of cells)	1.6	0.024
Highest volumetric activity (nmol/liter min)	530	25

[a] Data from the work of Oldenhuis (21) and Oldenhuis and Janssen (22).
[b] Highest degradation rate observed with washout occurring.

be caused by the fact that the measurements were done with whole cells and not with purified enzyme. Factors other than competition for the active site of the enzyme may influence the effect of toluene on TCE conversion and vice versa, e.g., reductant supply or substrate transport to the enzyme. With the same model, but using the K_m of toluene as the K_i on TCE conversion and vice versa, a washout of the system at TCE loading rates higher than 150 μmol/h was predicted (data not shown), indicating the necessity of using the measured values of the different constants in the model.

The model is based on the assumption that the growth yield of the cells on toluene is constant. This implies that TCE conversion does not affect the yield. However, it can be expected that this assumption no longer holds at high TCE loading rates, because TCE can become toxic to the cells and because TCE oxidation by toluene monooxygenase in *P. cepacia* G4 requires reducing equivalents. Nevertheless, the experimental results show that the assumption is applicable over a wide range of TCE loading rates.

A comparison of the measured and the predicted liquid phase concentrations shows that the latter are consequently higher. This can partly be explained by the sampling procedure. In the period needed to obtain a sample of the liquid phase from the chemostat, the conversion of both compounds certainly will proceed, which causes a significant reduction of the actual concentration. For an evaluation of the performance of the reactor system, however, these considerations are only of minor importance since the amounts of volatile compounds that left the system via the liquid were never more than 2 and 5% of the total load of toluene and TCE, respectively.

The potential volumetric activity of the chemostat is determined by the amount of biomass present in the system. In a cometabolic system, the latter is usually determined by the flux of the primary substrate through the reactor. Theoretically, a higher TCE conversion capacity can also be obtained by lowering the dilution rate of the fermentor, because this results in an increase in the amount of biomass. This was indeed observed after lowering the dilution rate from 0.08 to 0.04 h^{-1}. An additional advantage of such an approach is that a lower dilution rate results in a lower concentration of the growth-limiting substrate. Since toluene as the growth-limiting substrate inhibits the degradation of TCE, this suggests that the growth rate should be as low as possible. How low it may become is determined by the amount of chloride that is produced from TCE, since an increased residence time will result in accumulation of chloride in the chemostat.

The results obtained with *P. cepacia* G4 offer a good starting point for the development of an efficient bioreactor system for the microbial degradation of gaseous waste streams. The volumetric activities reported here are in the order of 0.8 to 4 g of TCE per m^3 per h and compare favorably with values of 0.06 to 0.6 g/m^3/h reported in the literature (9, 22, 28). In evaluating and comparing different systems, one should be aware that whether TCE is already dissolved in the aqueous phase or still has to be transferred from the gas phase may make a difference. The concentration range at which the system has to be effective also strongly affects the specific conversion rate. Recent legislation in western Europe requires TCE concentrations in off-gases to be below 100 mg/m^3.

ACKNOWLEDGMENT

This work was supported by a grant from the EC STEP program.

REFERENCES

1. **Alvarez-Cohen, L., and P. L. McCarty.** 1991. Effects of toxicity, aeration, and reductant supply on trichloroethylene transformation by a methanotrophic mixed culture. Appl. Environ. Microbiol. 57:228–235.
2. **Alvarez-Cohen, L., and P. L. McCarty.** 1991. A cometabolic transformation model for halogenated aliphatic compounds exhibiting product toxicity. Environ. Sci. Technol. 25:1381–1387.
3. **Alvarez-Cohen, L., and P. L. McCarty.** 1991. Two-stage dispersed growth treatment of halogenated aliphatic compounds by cometabolism. Environ. Sci. Technol. 25:1387–1393.
4. **Bailey, J. E., and D. F. Ollis.** 1986. Biochemical engineering fundamentals, 2nd ed. McGraw-Hill Kogakusha Inc., Tokyo.
5. **Broholm, K., T. H. Christensen, and B. K. Jensen.** 1992. Modelling TCE degradation by a mixed culture of methane-oxidizing bacteria. Water Res. 26:1177–1185.
6. **de Graaf, P. R.** Unpublished data.
7. **Ensley, B. D.** 1991. Biochemical diversity of trichloroethylene metabolism. Annu. Rev. Microbiol. 45:283–299.
8. **Ensley, B. D., and P. R. Kurisko.** 1994. A gas lift bioreactor for removal of contaminants from the vapor phase. Appl. Environ. Microbiol. 60:285–290.
9. **Ewers, J., D. Freier-Schröder, and H.-J. Knackmuss.** 1990. Selection of trichloroethylene (TCE) degrading bacteria that resist inactivation by TCE. Arch. Microbiol. 154:410–413.
10. **Folsom, B. R., and P. J. Chapman.** 1991. Performance characterization of a model bioreactor for the biodegradation of trichloroethylene by *Pseudomonas cepacia* G4. Appl. Environ. Microbiol. 57:1602–1608.
11. **Folsom, B. R., P. J. Chapman, and P. H. Pritchard.** 1990. Phenol and trichloroethylene degradation by *Pseudomonas cepacia* G4: kinetics and interactions between substrates. Appl. Environ. Microbiol. 56:1279–1285.
12. **Gossett, J. M.** 1987. Measurement of Henry's law constants for C_1 and C_2 chlorinated hydrocarbons. Environ. Sci. Technol. 21:202–208.
13. **Henry, S. M., and D. Grbić-Galić.** 1991. Influence of endogenous and exogenous electron donors and trichloroethylene oxidation toxicity on trichloroethylene oxidation by methanotrophic cultures from a groundwater aquifer. Appl. Environ. Microbiol. 57:236–244.
14. **Henschler, D.** 1985. Halogenated alkenes and alkynes, p. 317–347. *In* M. W. Anders (ed.), Bioactivation of foreign compounds. Academic Press, Inc., New York.
15. **Janssen, D. B., A. Scheper, L. Dijkhuizen, and B. Witholt.** 1985. Degradation of halogenated aliphatic compounds by *Xanthobacter autotrophicus* GJ10. Appl. Environ. Microbiol. 49:673–677.
16. **Janssen, D. B., A. Scheper, and B. Witholt.** 1984. Biodegradation of 2-chloroethanol and 1,2-dichloroethane by bacterial cultures. Prog. Ind. Microbiol. 20:169–178.
17. **Janssen, D. B., and B. Witholt.** 1992. Aerobic and anaerobic degradation of halogenated aliphatics, p. 299–327. *In* H. Sigel and A. Sigel (ed.), Metal ions in biological systems, vol. 28. Degradation of environmental pollutants by microorganisms and their metalloenzymes. Marcel Dekker, Inc., New York.
18. **Nelson, M. J. K., S. O. Montgomery, W. R. Mahaffey, and P. H. Pritchard.** 1987. Biodegradation of trichloroethylene and involvement of an aromatic biodegradative pathway. Appl. Environ. Microbiol. 53:949–954.
19. **Nelson, M. J. K., S. O. Montgomery, E. J. O'Neill, and P. H. Pritchard.** 1986. Aerobic metabolism of trichloroethylene by a bacterial isolate. Appl. Environ. Microbiol. 52:383–384.
20. **Nelson, M. J. K., S. O. Montgomery, and P. H. Pritchard.** 1988. Trichloroethylene metabolism by microorganisms that degrade aromatic compounds. Appl. Environ. Microbiol. 54:604–606.
21. **Oldenhuis, R.** 1992. Microbial degradation of chlorinated compounds. Ph.D. thesis. University of Groningen, Groningen, The Netherlands.
22. **Oldenhuis, R., and D. B. Janssen.** 1993. Degradation of trichloroethylene by methanotrophic bacteria, p. 121–133. *In* J. C. Murrell and D. P. Kelly (ed.), Microbial growth on C_1 compounds. Intercept Ltd., Andover, United Kingdom.
23. **Oldenhuis, R., J. Y. Oedzes, J. J. van der Waarde, and D. B. Janssen.** 1991. Kinetics of chlorinated hydrocarbon degradation by *Methylosinus trichosporium* OB3b and toxicity of trichloroethylene. Appl. Environ. Microbiol. 57:7–14.

STEROIDAL SAPONINS FROM THE LILIACEAE PLANTS AND THEIR BIOLOGICAL ACTIVITIES

Yoshihiro Mimaki and Yutaka Sashida

School of Pharmacy, Tokyo University of Pharmacy and Life Science, Tokyo 192-03, JAPAN

INTRODUCTION

The steroidal saponins are plant glycosides and they often possess properties such as froth forming, hemolytic activity, toxicity to fish, and complex formation with cholesterol. Some of the steroidal saponins isolated recently have been shown to be antidiabetic,[1] antitumor,[2] antitussive[3] and platelet aggregation inhibitors.[4] These reports have prompted us to carry out systematic studies on steroidal saponins of the Liliaceae and Agavaceae[5] plants. Our studies have resulted in the isolation of a number of new steroidal saponins including cholestane glycosides and steroidal alkaloids, some of which appeared to possess unique chemical structures and exhibited significant biological activities. In this review, we present steroidal compounds with novel structural features. The positive inotropic effects of steroidal and triterpene saponins associated with inhibition of cAMP phosphodiesterase (PDE) and antitumor activities of cholestane glycosides are also presented.

STEROIDAL COMPOUNDS WITH NOVEL STRUCTURAL FEATURES

Spirostanol Saponin with an HMG Group (1)

The genus *Allium* with *ca* 500 species has a wide distribution in the northern hemisphere and is known to be a rich source of steroidal saponins as well as sulfur-containing compounds. Although the *Allium* plants are classified to the family Liliaceae, because the flowers have superior ovaries, there are some botanists who have an opinion that they should be placed in Amaryllidaceae because of the umbellate inflorescence, while others weigh one opinion against another to classify them to their own family, Alliaceae.

Allium albopilosum is native to Turkestan and cultivated as an excellent cut flower. No publication can be traced concerning the steroidal saponins from *A. albopilosum*. Analysis of the bulbs of *A. albopilosum* led to the isolation of a novel steroidal saponin with a 3-hydroxy-3-methylglutaryl (HMG) group at the aglycone C-2 hydroxyl group (**1**).[6]

The absolute configuration of the asymmetric center of the HMG moiety was determined by the following chemical correlation. Alkaline methanolysis of **1** with 3% NaOMe in MeOH gave HMG monomethyl ester (**1a**). The methyl ester moiety of **1a** was reduced with $LiBH_4$ in THF at 0° for 3 h, and the reaction mixture was allowed to stand in acidic condition for 72 h to give (3*R*)-mevalonolactone (Figure 1). Thus, the asymmetric configuration of the HMG moiety was confirmed to be *S*.

Saponins Used in Traditional and Modern Medicine
Edited by Waller and Yamasaki, Plenum Press, New York, 1996

2 FPP → PSPP → squalene

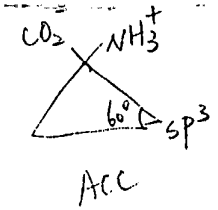

ACC

Fig. 26

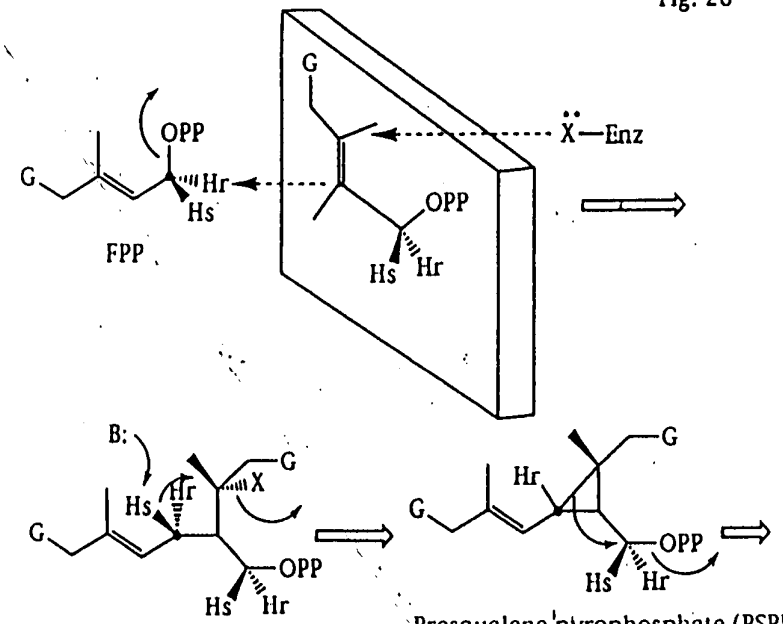

Presqualene pyrophosphate (PSPP) → 含一个 strain 很大的前鲨烯 三碳环分子

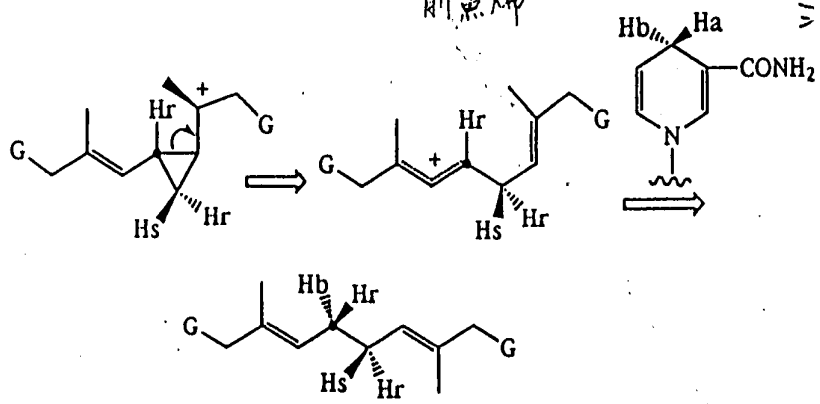

Squalene (G= Geranyl)

Fig. 26. Proposed mechanism for squalene formation catalyzed by squalene synthase.

△ 反应涉及2分子氧化態在经基階段的後相結合 (C-C bond formation from two carbinyl carbon), 此酶催化者乃一還原反应。

Fig. 27

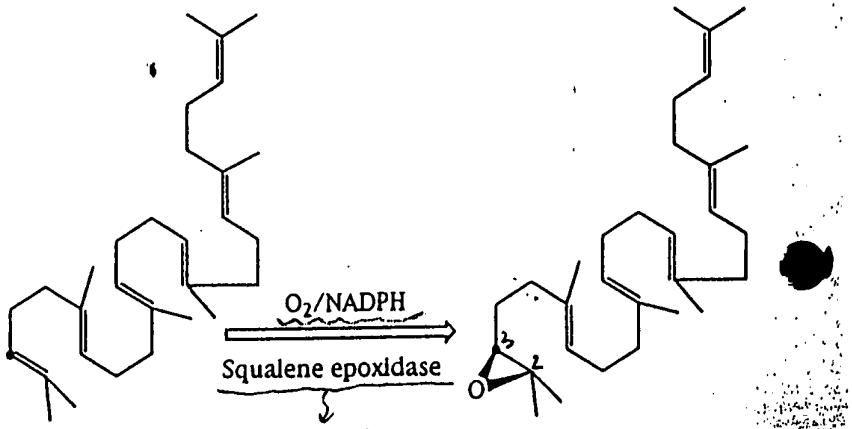

Fig. 27 Squalene epoxidase catalyses squalene to squalene epoxide.

△依熱力學考慮:

反应过程依序以 - P_iP_i release, cyclopropyl ring opening, allylic cation 之順序進行, Strain release 可能是統反应之 driving force 之一。